UNIVERSITY OF TWENTE.

Faculty of Electrical Engineering,
Mathematics & Computer Science

Design of an RF receiver in BiCMOS implementing beamforming to reject interference

E.M. Kleinsmann
MSc. Thesis
April 2013

Supervisors:
prof. dr. ir. B. Nauta
dr. ing. E.A.M. Klumperink
dr. ir. A.B.J. Kokkeler
ir. R.E. Struiksma

Report number: 067.3503
Chair of Integrated Circuit Design
Faculty of Electrical Engineering,
Mathematics & Computer Science
University of Twente
P.O. Box 217
7500 AE Enschede
The Netherlands

Abstract

This thesis deals with the implementation of an RF frontend for a digital beamforming Software Defined Radio receiver. Initial beamforming is implemented in the frontend to reject interferers, which would otherwise desensitise the frontend.

A beamforming strategy is presented which creates a beam by applying independent phase shifts to the input signals. This way the radiation pattern of the beam is altered resulting in varying beamshapes and differently placed zeros. This beam is then used to create a set of 4 orthogonal beams, which, together, prove to preserve all information, so further beamforming can be performed in software. Interferers can be rejected in the frontend by 'capturing' the interferer in 1 of the 4 beams, therewith not affecting the other 3 beams.

A circuit level implementation re-using the LO phases already created for harmonic rejection to implement beamforming and therewith saving the implementation of extra phase shifters is proposed.

Circuit simulation shows an improvement of the signal-to-interferer ratio of the created beams by 14 to 33 dB in a worst-case scenario in comparison to when no initial beamforming is implemented in the frontend.

Acknowledgements

First of all, I would like to offer my gratitude to my supervisor, Eric Klumperink, who has provided me with this assignment and has supported me throughout my thesis with his knowledge and patience, allowing me to work on this thesis in my own pace.

Secondly, I would like to thank Remko Struiksma for his useful advices during the work on this research and his feedback on the writing of this thesis. Also I am thankful to André Kokkeler for taking place in my graduation committee. Furthermore, I would like to acknowledge Bram Nauta for helping out at the last moment and leading my graduation committee. I would also like to express my gratitude to Gerdien Lammers for helping me out with carrying out all the administrative tasks required for my graduation.

Finally, my thanks goes out to my family who have always supported me throughout my studies.

Table of contents

Acronyms

ADC	Analogue-to-Digital Converter
DSP	Digital Signal Processor
FOM	Figure Of Merit
IF	Intermediate Frequency
LNA	Low-Noise Amplifier
LO	Local Oscillator
RF	Radio Frequency
SDR	Software Defined Radio
SNR	Signal-to-Noise Ratio

Mathematical symbols

$\overline{f(x)}$	Complex conjugate of $f(x)$
$\lvert f(x) \rvert$	Absolute value of $f(x)$
$\lVert f(x) \rVert$	Norm of $f(x)$
:	Such that
$\{ : \}$	The set of ... such that
$\forall$	For all
$\exists$	There exists
$\in$	Is an element of
$\notin$	Is not an element of
$\mathbb{Z}$	The set of integers
$\mathbb{R}$	The set of real numbers
$\mathbb{C}$	The set of complex numbers
$\Re\{f(x)\}$	The real part of $f(x)$
$\Im\{f(x)\}$	The imaginary part of $f(x)$
■	End of proof
$\wedge$	Logical conjunction

List of figures

List of tables

1 Introduction

The present-day radio frequency spectrum is becoming more and more filled with communication systems operating in the same frequency region. Therefore, receivers have to be equipped with highly selective analogue frequency filters. Some frequency bands, such as the 2.4GHz section of the S band, are becoming increasingly cluttered and as a result frequency filtering often proves insufficient (Jing Zhu 2007). As an example consider the overlapping Wi-Fi channels shown in Figure 1. Due to the partial overlap the wanted signal and the interferer cannot be separated in the frequency domain. And thus, a strong interferer in a close channel can overpower the wanted signal. Therefore, a different filtering technique is desired.

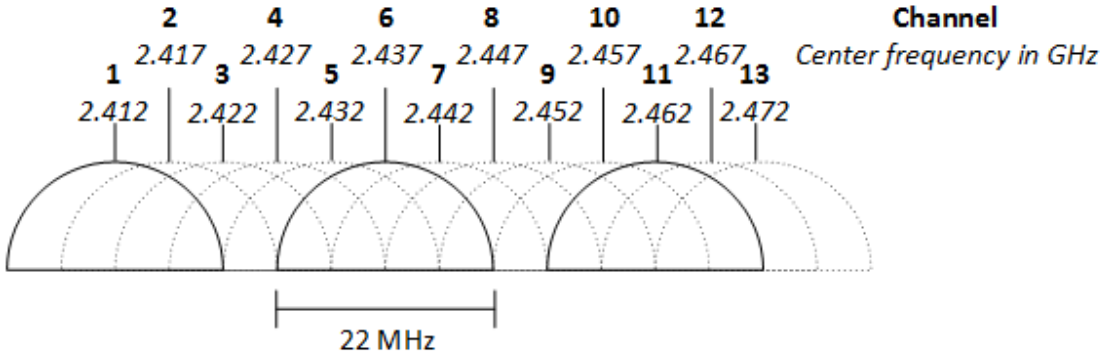

Figure 1: Overlapping Wi-Fi___33 channels in the frequency spectrum.

Another way to distinguish between two signals is to use beamforming (spatial or directional filtering). That is, use the angle of arrival to differentiate between signals. Figure 2 illustrates the concept of spatial filtering. The plot displays the sensitivity of a spatial filter as a function of the angle of arrival of the signal. For certain directions the filter has a low sensitivity and interferers originating from that direction will be rejected.

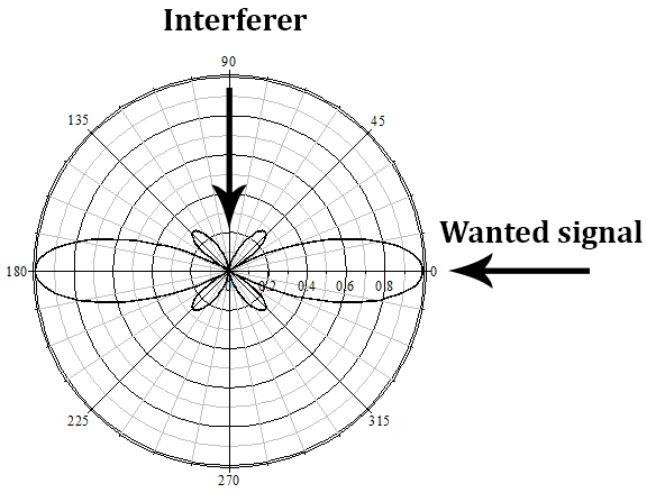

Figure 2: The concept of spatial filtering.

The directional dependence of the strength of the radio waves an antenna transmits or receives is called the radiation pattern of an antenna. Regardless of whether an antenna is used as a transmitting or a receiving antenna its radiation pattern is identical because of the reciprocity theorem (Visser 2005, 101-102).

Beamforming is done by combining the signals from an array of antennas to construct a new signal: a beam. The beam constructed of this antenna array will have a radiation pattern different from the radiation pattern of the individual elements. That is, the antenna array can be used to create a spatial filter. As an example the beam constructed by summing the signals of a 4-element array can be seen in Figure 3.

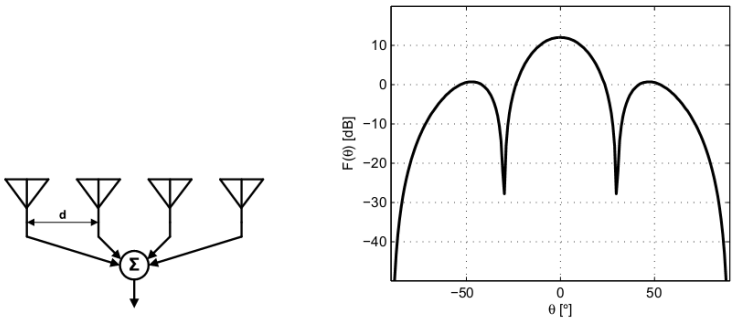

Figure 3: Combining an antenna array (left) and the radiation pattern (right) of the constructed beam.

Modern communication systems, such as a mobile phone, incorporate an increasing amount of communication standards. And as such these systems need more and more hardware. Therefore, a lot of research is conducted in the field of Software-Defined Radio (SDR). In a SDR system, components traditionally implemented in hardware are implemented in software. And, consequently, SDR systems result in a much more flexible and adaptable system (Buracchin 2000).

Steep and adaptable spatial filters are difficult to implement in analogue hardware and could therefore benefit greatly from an implementation in software. Such a system would still need interfacing to the antennas, that is, a radio frequency frontend, though (STARS - Theme 2: Analog Front-Ends 2013).

1.1 Project description

The goal of this research is to design an RF frontend for digital beamforming SDR systems. Software defined spatial filtering could provide a very flexible system. Since interferers can originate from any angle, often needing differently configured spatial filters, flexibility makes for a big advantage of digital spatial filtering.

For software defined spatial filtering to be possible the signal needs to be available to the digital signal processing core (DSP), though. Therefore the signal has to be converted by an analogue-to-digital-converter (ADC). Yet, it is not possible to pass the signals from the antennas directly to the ADC due to unfeasible requirements for the ADC (Klumperink 2007). An RF frontend is thus needed to pre-process the signal.

Apart from amplifying the input signals and bringing them down to a lower frequency, it might also be beneficial to perform some initial beamforming in this frontend. The reason for this is that there may be such a strong interferer that proper conversion by the ADC is not possible and the input signal would be heavily distorted.

To illustrate this problem consider the system in Figure 4. The system is an RF frontend interfacing to a 4-element array. A very strong interferer is present and the signals of all antennas are too large for the ADC. The signals of all 4 antennas are distorted as can be seen in Figure 4. Filtering out the interferer by digital beamforming does not solve this problem, because the RF frontend is already desensitised by the interferer.

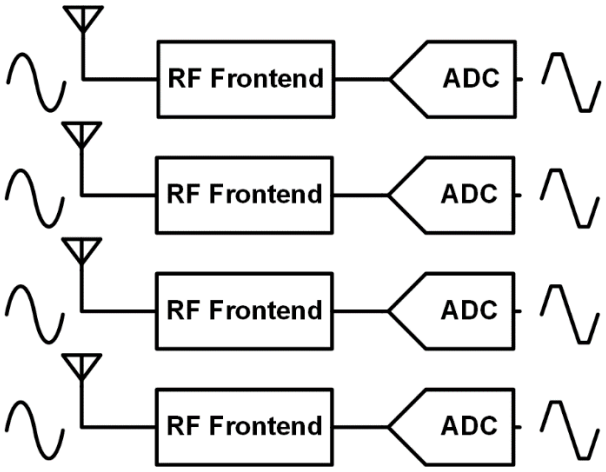

Figure 4: RF Frontend interfacing to a 4-element antenna array.

Now consider Figure 5 where 4 beams are constructed before the input signals pass the ADCs. The strong interferer is only present in one of the beams and as a result only one of the 4 input signals is distorted. So, initial beamforming in the frontend could reduce the total distortion of the system.

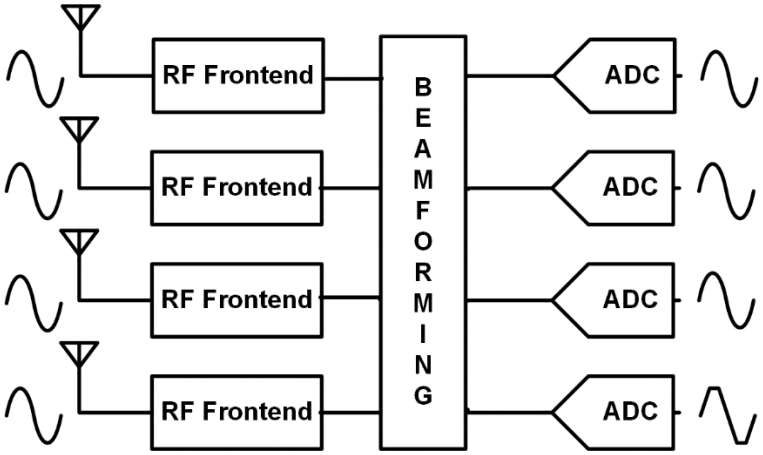

Figure 5: RF Frontend with beamforming interfacing to a 4-element antenna array.

Multiple different beamforming strategies in the frontend are possible and are investigated in this thesis.

So, the RF frontend should pre-process the input signals as to ensure proper conversion by the ADC. That is, the input signals have to be amplified and mixed down to base band. Furthermore, some initial beamforming should be implemented to prevent the frontend from desensitizing by strong interferers.

Desensitisation of the frontend, which leads to distortion of the input signals, could also be prevented by attenuating the input signals. If the interferer is much stronger than the wanted signal, though, the wanted signal will only span a small part of the voltage range of the ADC. Thus, the resolution of the ADC for the wanted signal is effectively lowered and therewith the SNR of the wanted signal.

This MSc thesis is a part of a research at the University of Twente that seeks to implement a reconfigurable receiver in a BiCMOS technology. BiCMOS offers good RF performance, while also being cost-effective. And as such the receiver proposed in this thesis will also be designed in BiCMOS.

To sum up, the aim of this MSc thesis project is threefold.

1. Analyse different possible strategies for beamforming in the frontend and the benefits these could achieve.
2. Design a receiver in BiCMOS as frontend that implements the best beamforming strategy.
3. Verify the performance of the receiver by circuit simulations.

1.2 Overview of a typical RF frontend

As stated in the previous section the main goal of this research is the design of an RF frontend for an SDR beamforming system. An overview of the functions of a typical RF frontend are described in this section. As well as the building blocks typically used to achieve these functions.

The two key functions of a receiver are amplifying the input signal and mixing the input signal down from a high radio frequency to a low base band frequency. Traditionally, the input signal would be amplified first and then mixed down to base band. Nowadays, those functions can be performed in either order, though.

The amplification of the input signal is usually carried out by a low-noise amplifier (LNA). The frequency translation of the input signal, the mixing down, is performed by the mixer. The mixer is basically a multiplier and needs another signal, the local oscillator (LO), to multiply the input signal with. The LO is normally electronically tuneable by the means of a voltage controlled oscillator (VCO). And finally, any unwanted frequencies are filtered out by a frequency filter. The input signal is then suitable to be passed through the ADC. Any additional signal processing, such as demodulation and beamforming, can then be performed by a digital signal processor (DSP).

The complete analogue frontend represented in a block diagram can be seen in Figure 6.

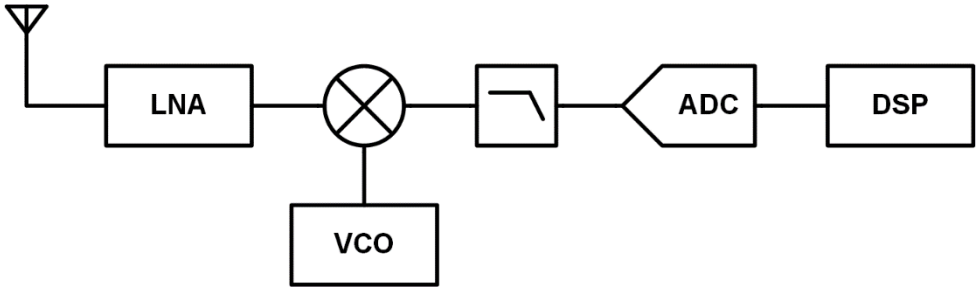

Figure 6: Block diagram of a typical RF receiver.

In this thesis the option is explored to implement beamforming at IF, after downmixing. Thus, beamforming implemented in or after the mixer. Therefore this research will focus on the implementation of the mixer block of the RF frontend.

1.3 Beamforming

This section gives a short introduction to beamforming and describes the core principle it is based upon. Furthermore, the 4-element linear array antenna that will be used in this research is described.

An antenna array is a group of two or more *radiators* or *elements* whose currents differ in amplitude and/or phase. These elements can be used to improve the directivity of an antenna system and make it electronically steerable. Its ability to improve the radiated signal in the desired direction, while mitigating it in the non-desired direction is founded in electromagnetic wave interference phenomena.

The analysis of beamforming in this chapter is partly based on (Visser 2005, 123-131).

1.3.1 Linear array antenna

When the radiators are arranged in a straight line the system is called a *linear array antenna*. For the analysis of such a system these radiators are assumed to be identical and placed equidistantly. Moreover, the radiators are assumed to be point sources and the array antenna is considered to be a receiving antenna.

A wave is a disturbance or oscillation in both space and time. It can be described by its wave function

$$s(t) = A\cos(\omega t \pm kl) = A\Re\{e^{\omega t \pm kl}\} \tag{1.1}$$

Where ω is the angular frequency of the signal $s(t)$, A the amplitude of the signal and l is the distance along the propagation path. k is the wave number and is defined as:

$$k = \frac{2\pi}{\lambda} \tag{1.2}$$

Where λ is the wavelength of the signal $s(t)$.

The phase, $\Phi(t)$, of signal $s(t)$ is given by

$$\Phi(t) = \omega t \pm kl \tag{1.3}$$

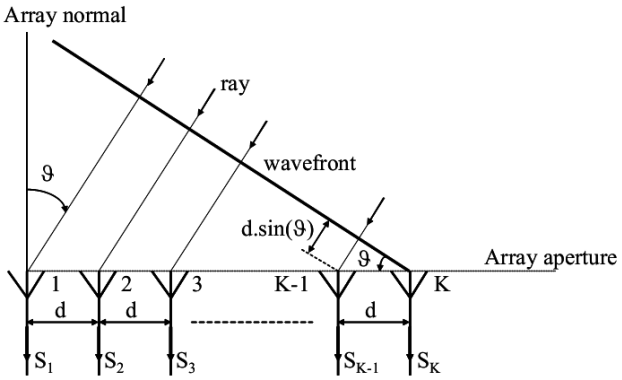

Figure 7: A linear array of K radiators.

Now, consider the system in Figure 7 and assume that the wavefront of a plane wave is incident upon this system under an angle θ with the array normal. The definition of a wavefront dictates that all points in space on the wavefront have identical amplitude and phase values. Although the wavefront of a real-life antenna at a large distance would most likely be spherical, the wavefront can be regarded locally planar because of the array's finite size.

The wavefront will first reach element K. At that moment the wavefront has to travel another distance $\mathrm{d} \cdot \sin(\theta)$ to arrive at element $K-1$. For each consecutive element the wavefront has to travel another time that distance. So, for the wavefront to reach element i, where $i \in \mathbb{N} : i \leq K$ it has to travel a distance $(K-i) \cdot d \cdot sin(\theta)$, after reaching element K. Substituting this distance in equation 1.3 the following equation is distilled for the phase at element i:

$$\Phi_i(t) = \omega t \pm k_0(K-i) \cdot d \cdot sin(\theta) \tag{1.4}$$

Where k_0 is the wave number in free space.

The complex signal, denoted by S_i, received by the elements of the array may now be expressed as

$$S_i(t,\theta) = S_e(\theta) a_i e^{jk_0(K-i)\cdot d\cdot sin(\theta)} e^{j\omega t} \tag{1.5}$$

Where $S_e(\theta)$ is the radiation pattern of a single, isolated radiator of the antenna array, also known as the element factor; a_i is the amplitude of the received signal by element i.

In this thesis a couple of simplifying assumptions will be used:

- The amplitude of the received signals on all elements is equal and normalised. That is,

$$a_i = 1 \; for \; i \in \mathbb{N} : i \leq K \tag{1.6}$$

- The elements have no mutual coupling and are isotropic. That is,

$$S_e(\theta) = 1 \tag{1.7}$$

- The time dependence is omitted, because it would appear in every equation and plays no role in beamforming.

Under these assumptions equation 1.5 is reduced to:

$$S_i(\theta) = e^{jk_0(K-i)\cdot d\cdot sin(\theta)} \tag{1.8}$$

The sum of all elements of the array, without applying any weighting, is the aforementioned array factor.

$$S(\theta) = S_a(\theta) = \sum_{i=1}^{K} e^{jk_0(K-i)\cdot d\cdot sin(\theta)} \tag{1.9}$$

The normalised power radiation pattern of the antenna array, which is later on used to define a figure of merit, can be calculated by

$$P(\theta) = \frac{1}{K}|S(\theta)| \tag{1.10}$$

1.3.2 Linear broadside array antenna

For this research an antenna array consisting of 4 radiators with an inter-element spacing of half a wavelength in free space is assumed. That is,

$$K = 4 \tag{1.11}$$

$$d = \frac{\lambda_0}{2} \tag{1.12}$$

Substituting these values in equation 1.9 gives the following radiation pattern.

$$S(\theta) = S_a(\theta) = \sum_{i=1}^{4} e^{j\pi(K-i)sin(\theta)} \tag{1.13}$$

This system is called a linear broadside array antenna and a plot of its normalised power radiation pattern can be seen in Figure 8. The plot shows that, while the radiators forming the array are isotropic, the array antenna as a whole clearly is not. Waves with an angle of incidence of $\pm$90° and $\pm$30° are nullified by the array antenna –or– the array antenna has zeros at $\pm$90° and $\pm$30°. The area between -30° and 30°, where the beam has its maximum, is called the main lobe of the beam. The other lobes at $\pm$50° are called side lobes.

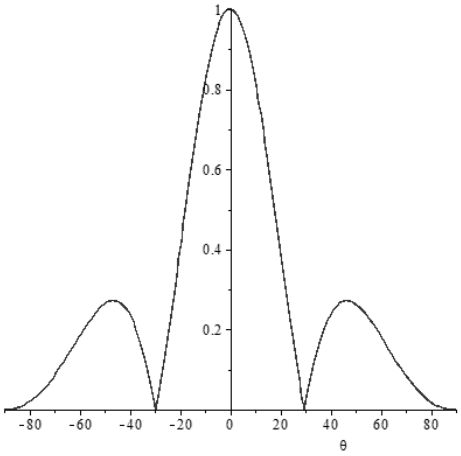

Figure 8: Plot of radiation pattern of broadside array antenna.

Radiation patterns are generally displayed in the so-called u-space. That is, plotted with respect to the variable u, which is defined as

$$u = \sin(\theta) \tag{1.14}$$

The main reason for this convention is that the beamshape is invariant when shifted in u-space, whereas it is not with respect to the angle θ. An example to illustrate this is shown in Figure 9. Therefore, from here on in, all expressions are denoted as functions of u, rather than θ.

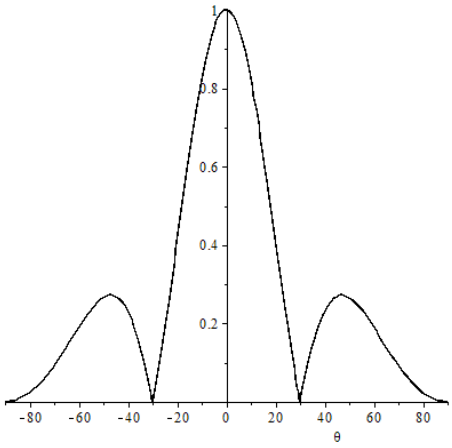

a. Radiation pattern broadside array antenna.

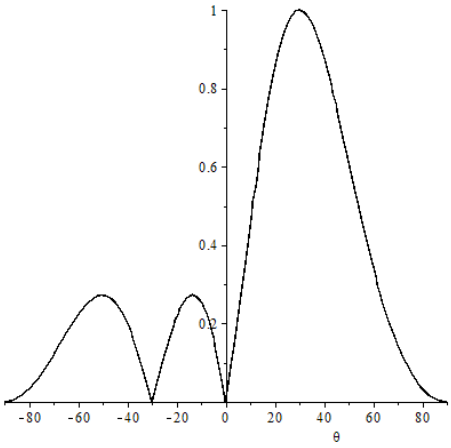

b. Radiation pattern broadside array antenna shifted by 30°.

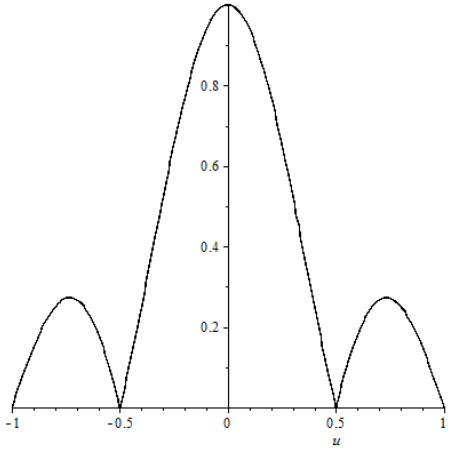

c. Radiation pattern broadside array antenna in u-space.

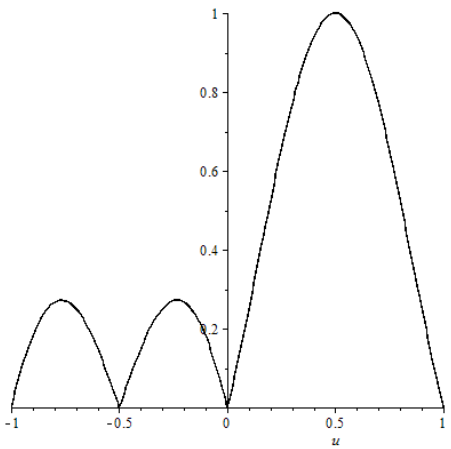

d. Radiation pattern broadside array antenna schifted 0.5 in u-space.

Figure 9: The beamshape is invariant when shifted in u-space.

1.3.3 Beamforming

It is possible to alter the radiation pattern of a linear array antenna by amplifying and/or phase shifting the signals from the separate radiators before summing them. Mathematically, this means that the signals are weighted with complex weights prior to summing them. That is,

$$S(u) = S_a(u) = \sum_{i=1}^{4} a_i e^{j\pi(K-i)u} \tag{1.15}$$

Where the complex weights a_i are of the form

$$A, \phi \in \mathbb{R} : a_i = Ae^{j\phi} \tag{1.16}$$

In which A is the amplification and ϕ the phase shift. The radiation pattern that is constructed this way is called a *beam* and the process of forming such a beam is titled *beamforming.*

1.3.4 Mathematical properties of beamforming patterns

Though, mathematically apparent, two properties of beamforming patterns are explicitly stated in this section, since they will be used in subsequent chapters.

1. *Any common phase shift applied to the separate radiator signals will not affect the power radiation pattern of the array antenna.*

Consider weights of the following form

$$a_i = e^{j(\phi_i + \psi)} \tag{1.17}$$

Where ϕ_i is the phase shift applied to the signal of element i and ψ is some common phase shift that is applied to all element's signals.

Then,

$$\begin{aligned} |S(u)| &= \left|\sum_{i=1}^{4} e^{j(\phi_i+\psi)} \cdot e^{j\pi(K-i)u}\right| \\ &= \left|e^{j\psi}\right| \cdot \left|\sum_{i=1}^{4} e^{j\phi_i} \cdot e^{j\pi(K-i)u}\right| \\ &= 1 \cdot \left|\sum_{i=1}^{4} e^{j\phi_i} \cdot e^{j\pi(K-i)u}\right| \blacksquare \end{aligned} \tag{1.18}$$

2. *To shift the radiation pattern with respect to u, a phase shift proportional to $\pi(K-i)$ should be applied to all signals*.

Consider weights of the following form

$$a_i = e^{j(\phi_i + \pi(K-i)v)} \tag{1.19}$$

Where ϕ_i is the phase shift applied to the signal of element i and v is the desired shift in u-space.

Then,

$$S(u+v) = \sum_{i=1}^{4} e^{j(\phi_i + \pi(K-i)v)} \cdot e^{j\pi(K-i)u} \tag{1.20}$$

$$= \sum_{i=1}^{4} e^{j\phi_i} \cdot e^{j\pi(K-i)(u+v)} \blacksquare$$

1.4 Mixer

In chapter 4 the implementation of beamforming using the extra LO phases for harmonic rejection mixing is considered. This section gives a short introduction to mixers, explains why harmonic rejection is desirable and describes the core principle of harmonic rejection.

An essential component of the receiver is the mixer. It takes care of the frequency translation of the input signal from RF to baseband. Ideally, the mixer would perform this frequency translation without generating any unwanted signals. This would be the case if the frequency translation would be carried out by an ideal multiplier. Mixers perform the multiplication operation, but they are not ideal and other unwanted signals are produced in the process.

The translation in the frequency domain is performed by the multiplication of two signals in the time domain. Consider the following two signals.

$$a(t) = \cos(\omega_a \cdot t) \tag{1.21}$$

$$b(t) = \cos(\omega_b \cdot t) \tag{1.22}$$

Now, the product of these two signals is

$$a(t) \cdot b(t) = \frac{1}{2}\cos((\omega_a - \omega_b) \cdot t) + \frac{1}{2}\cos((\omega_a + \omega_b) \cdot t) \tag{1.23}$$

And, as can be seen, a frequency translation both up and down has taken place. This is the core principle all mixers are based on.

Nowadays, the vast majority of the mixers implemented in receivers are switching mixers. These mixers carry out the multiplication by commutating either a current or voltage. That is, the input signal is multiplied by a square wave. This multiplication by a square wave instead of a sinusoid leads to the creation of unwanted signals. This can be explained by looking at the Fourier series representation of a square wave, below.

$$p_0(t) = \frac{4}{\pi} \cdot \left(\cos(\omega t) - \frac{1}{3}\cos(3\omega t) + \frac{1}{5}\cos(5\omega t) - \frac{1}{7}\cos(7\omega t) + \cdots\right) \tag{1.24}$$

A square wave is made up by one fundamental sinusoid and an infinite number of odd harmonics. So, multiplying with a square wave does not only result in a frequency translation by $\pm\omega$, but also by $\pm 3\omega$, $\pm 5\omega$, $\pm \cdots$, resulting in up/down converting unwanted frequency bands.

1.4.1 Harmonic rejection mixer

A harmonic rejection mixer suppresses harmonic mixing by one or more dominant harmonics. This is done by not multiplying with a single square wave, but effectively by a stair-case approximation of a sine, which can be constituted

from summing square waves with different phases. Once again, the Fourier series representation of a square wave can explain this.

Consider $p_{-45}(t)$ and $p_{45}(t)$, a -45 degrees and +45 degrees phase-shifted copy of $p_0(t)$, respectively. Its Fourier expansion can be obtained from equation 1.24 and can be seen in equation 1.25 and 1.26.

$$\begin{aligned} \mathrm{p}_{-45}(\mathrm{t}) &= \mathrm{p}_0\left(\mathrm{t}-\tfrac{\pi}{4\omega}\right) \\ &= \frac{4}{pi}\Big[\left(\cos\left(\omega t-\frac{\pi}{4\omega}\right)-\frac{1}{3}\cos\left(3\omega t-\frac{\pi}{4\omega}\right)+\frac{1}{5}\cos\left(5\omega t-\frac{\pi}{4\omega}\right)\right. \\ &\qquad \left.-\frac{1}{7}\cos\left(7\omega t-\frac{\pi}{4\omega}\right)+\cdots\Big] \\ &= \frac{2\sqrt{2}}{\pi}\Big[\left(\cos(\omega t)+\sin(\omega t)\right)+\frac{1}{3}\left(\cos(3\omega t)-\sin(3\omega t)\right) \\ &\qquad -\frac{1}{5}\left(\cos(5\omega t)-\sin(5\omega t)\right)-\frac{1}{7}\left(\cos(7\omega t)-\sin(7\omega t)\right)+\cdots\Big] \end{aligned} \tag{1.25}$$

$$\begin{aligned} \mathrm{p}_{-45}(\mathrm{t}) &= \mathrm{p}_0\left(\mathrm{t}+\tfrac{\pi}{4\omega}\right) \\ &= \frac{4}{pi}\Big[\left(\cos\left(\omega t+\frac{\pi}{4\omega}\right)-\frac{1}{3}\cos\left(3\omega t+\frac{\pi}{4\omega}\right)+\frac{1}{5}\cos\left(5\omega t+\frac{\pi}{4\omega}\right)\right. \\ &\qquad \left.-\frac{1}{7}\cos\left(7\omega t+\frac{\pi}{4\omega}\right)\Big] \\ &= \frac{2\sqrt{2}}{\pi}\Big[\left(\cos(\omega t)-\sin(\omega t)\right)+\frac{1}{3}\left(\cos(3\omega t)+\sin(3\omega t)\right) \\ &\qquad -\frac{1}{5}\left(\cos(5\omega t)+\sin(5\omega t)\right)-\frac{1}{7}\left(\cos(7\omega t)+\sin(7\omega t)\right)+\cdots\Big] \end{aligned} \tag{1.26}$$

Now, if $p_0(t)$ is scaled by $\sqrt{2}$ and summed with $p_{-45}(t)$ and $p_{45}(t)$, a staircase signal is created (equation 1.27).

$$\begin{aligned} \mathrm{p}_{\mathrm{HR}}(\mathrm{t}) &= \sqrt{2}\cdot\mathrm{p}_0(\mathrm{t})+\mathrm{p}_{-45}(\mathrm{t})+\mathrm{p}_{45}(\mathrm{t}) \\ &= \frac{8\sqrt{2}}{\pi}\left[\cos(\omega t)-\frac{1}{7}\cos(7\omega t)+\cdots\right] \end{aligned} \tag{1.27}$$

Every third and fifth harmonic is cancelled for this newly created signal. This is the core principle harmonic rejection mixing is based upon as was first described in (J. A. Weldon 2001).

Since the output of the mixer is shifted by the phase of the supplied LO signal, the extra LO phases for harmonic rejection can also be used for phase shifting. These mixers are therefore later on also called LO phase shifters.

Figure 10 shows a graphical representation of harmonic rejection. The staircase signal contains no third and fifth harmonic. And, as such, these are not mixed to the output.

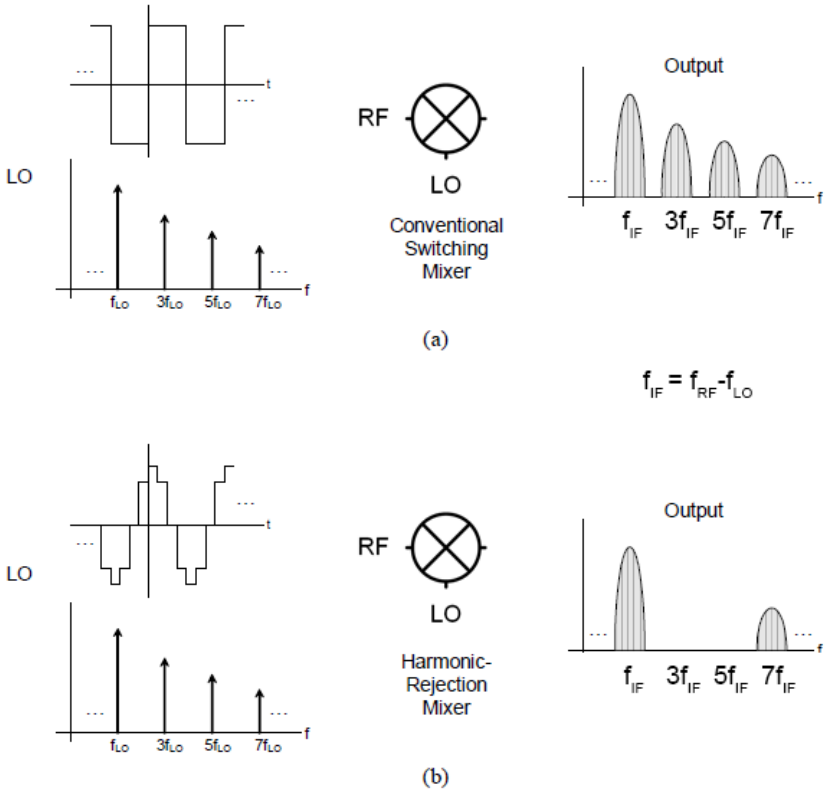

Figure 10: (a) Input, LO and output of a conventional switching mixer. (b) Input, LO and ouput of a HR switching mixer. (J. Weldon 2005)

There is one caveat, though. It is difficult to realize a ratio of $\sqrt{2}$ to 1 on-chip, because of mismatch between devices in production. The best results are obtained when unit cells are used, which require a rational approximation. This thesis will use a ratio of 7:5, accurate within 1%. Better approaches exist such as the two-stage solution demonstrated in (Ru, et al. 2009).

1.5 Previous work

In previous work (Paramesh 2005) a beamforming system based upon a vector modulator was proposed. The vector modulator interpolates between quadrature phases to perform phase shifting and/or amplification. This concept is illustrated in Figure 11. The quadrature phases I & Q are summed with adjustable weights to achieve different phase shifts. The resulting vectors are then summed. That is, the input signals are summed with complex weights to form a beam.

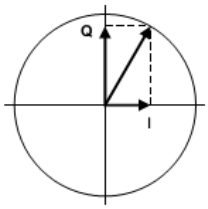

Figure 11: Vector modulation using quadrature phases.

In (van den Ende, et al. 2011) a beamforming algorithm based upon a Butler Matrix beamforming network was investigated and implemented using op-amps and resistors that can be seen in Figure 12.

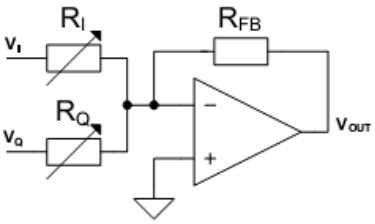

Figure 12: Vector modulator implementation proposed in (van den Ende, et al. 2011).

The strategy for beamforming that was used is called beamsteering. This strategy uses one fixed beamshape, that of the Butler Beams, and shifts it in u-space to achieve zeros in different angles.

In this thesis the strategy of using one fixed beamshape is compared against a strategy using variable beamshapes. Furthermore it is explored if the extra LO phases created for harmonic rejection can also be used to implement one of these beamforming strategies and therewith saving the implementation of dedicated phase shifters for beamforming.

1.6 Research questions

1. How does the beamsteering –or– fixed beamshape strategy used in (Paramesh 2005) and (van den Ende, et al. 2011) perform against a strategy using variable beamshapes?

2. Is it feasible to implement beamforming using only the LO phase shifters created for harmonic rejection? Which extra hardware needs to be implemented?

3. What is the performance of the beamforming strategy when implemented in a BiCMOS process? And, what is the performance of the mixer implementing beamforming?

1.7 Outline

This thesis is arranged as follows:

- Chapter 2 introduces a method to construct a beam basis. That is, a set of beams that can be used to construct any other beam.
- Chapter 3 describes two beamforming strategies that can be used to implement beamforming.
- Chapter 4 evaluates the performance of both beamforming strategies using a numerical analysis simulation method.
- Chapter 5 proposes a circuit level design implementing beamforming.
- Chapter 6 evaluates the performance of the circuit level design using simulation results of SpectreRF.
- Chapter 7 presents the conclusions.
- Chapter 8 offers some recommendations.
- Appendix A shows the MATLAB code that was used to conduct the numerical analysis described in chapter 4.

2 The construction of a beam basis

As discussed earlier the signals from the radiators are summed with complex weights. These weights can be adjusted to achieve different radiation patterns. The signal that is created by the weighted summation of the signals of the array is called a beam. By forming a beam information is lost. Any signal coming from a direction where the radiation pattern of the beam has a zero is lost. Since the real spatial filtering will be performed in the software it is of crucial importance that all information is kept or at least as much of it as possible. Therefore, multiple beams have to be constructed, which, together, will contain all information.

In this chapter a method to construct a set of orthogonal beams is derived. Furthermore, it is proven that this set is a basis for the set of all beams –or– beam basis. That is, a method is described to form a set of beams that can form any other beam by a linear combination of these beams.

2.1 The function set of all beams

Let S be the function space containing all beams that can be formed by summing the signals of a 4-element array antenna with complex weights. This function space can be defined as

$$S = \left\{ f(u) \in L^2(-1,1) : f(u) = \sum_{i=1}^{4} a_i \cdot e^{j\pi(4-i)u} \right\}_{a_i \in \mathbb{C}} \tag{2.1}$$

Where L^2 is the set of square-integrable functions and a_i is some arbitrary constant. The domain of the function space is restricted to L^2 to ensure an inner product exists. Furthermore, the function space is restricted to the interval $[-1,1]$, because $u \in [-1,1]$. Since S is a closed set and a subspace of L^2-space it is a Hilbert space. Therefore there exists an orthonormal basis $\{f_i\}_{i\in\mathbb{N}}$ and the following are equivalent (Griffiths 2005, 93-96)

1. $\{f_i\}_{i\in\mathbb{N}}$ is an orthonormal basis for H (2.2)
2. $\forall g \in S : g = \sum_{i\in\mathbb{N}} \langle g, f_i \rangle \cdot f_i$ (2.3)
3. $\forall i : \langle x, f_i \rangle = 0 \longrightarrow x = 0$ (2.4)

Where $\langle \cdot, \cdot \rangle$ is the inner product, which, in this context, is defined as

$$\langle g, f \rangle = \int_{-1}^{1} g(u) \cdot \overline{f(u)} \cdot du \tag{2.5}$$

Where g and f are two complex functions on the closed interval $[-1,1]$.

A basis for function space S is a set of orthogonal functions that, in a linear combination, can represent any function in S. For a basis to be an orthonormal basis the following condition needs to be met.

$$\forall i : \|f_i\| = \sqrt{\langle f_i, f_i \rangle} = 1 \tag{2.6}$$

It is easily verifiable that the set of the input functions of a 4-element array antenna, H, is a basis for S, where H is defined as

$$H = \left\{ f(u) \in L^2(-1,1) : f(u) = e^{j\pi i u} \right\}_{i \in \{0,1,2,3\}} \tag{2.7}$$

And H' is an orthonormal basis for S, where H' is defined as

$$H' = \left\{ f(u) \in L^2(-1,1) : f(u) = \frac{1}{\sqrt{2}} e^{j\pi i u} \right\}_{i \in \{0,1,2,3\}} \tag{2.8}$$

2.2 The construction of a basis for the function set of all beams

For no information to be lost the beams formed in the analogue frontend should also form a basis for S. As stated earlier the beams formed in the frontend are of the following form

$$f(u) = \sum_{i=1}^{4} a_i e^{j\pi(4-i)u} \tag{2.9}$$

Now, a set of orthogonal beams has to be found, that will form a basis, B, for function space S. Since all functions in B should be mutually orthogonal the following is true

$$f_i, f_j \in B \wedge i \neq j : \langle f_i, f_j \rangle = 0 \tag{2.10}$$

Equation 2.10 can be used to find a possible basis for S. Let $f'(u, v)$ be a copy of $f(u)$ shifted by v with respect to u, that is,

$$f'(u, v) = \sum_{i=1}^{4} a_i e^{j\pi(4-i)(u+v)} \tag{2.11}$$

Then, the solution to the following equation yields all possible values for v, for which $f'(u, v)$ is orthogonal to $f(u)$

$$\langle f, f' \rangle = \int_{-1}^{1} \sum_{i=1}^{4} a_i e^{j\pi(4-i)u} \cdot \overline{\sum_{\iota=1}^{4} a_\iota e^{j\pi(4-\iota)(u+v)}} \cdot du = 0 \tag{2.12}$$

This can be reduced to:

$$\sum_{i=1}^{4} |a_i|^2 \cdot e^{-j\pi i v} = 0 \tag{2.13}$$

With the solution:

$$\text{If } |a_i| = 1 \text{ then } n \in \left\{ n \in \mathbb{Z} : \frac{n}{4} \notin \mathbb{Z} \right\} : \; v = \frac{n}{2} \tag{2.14}$$

As e^{jx} is periodic with period 2π, only 3 solutions of v are admissible for basis B, since all functions in the basis should be mutually orthogonal.

Now, a possible basis B for S can be constructed

$$B = \left\{ f(u,v) = C \cdot \sum_{i=1}^{4} a_i e^{j\pi(4-i)\left(u+\frac{v}{2}\right)} : |a_i| = 1 \right\}_{v\in\{0,1,2,3\}} \tag{2.15}$$

Where C is some normalisation constant to make basis B an orthonormal basis. To proof that basis B is indeed an orthonormal basis for S equation 2.3 can be used. This yields the following equation

$$\forall g \in S, f_v \in B : \sum_{v=1}^{4} \int_{-1}^{1} g(u) \cdot f_v(u,v) \cdot du \cdot f_v(u,v) = g(u) \tag{2.16}$$

Filling in the expressions for g and f_v yields

$$\sum_{v=1}^{4} \int_{-1}^{1} \sum_{i=1}^{4} b_i \cdot e^{j\pi(4-i)u} \cdot C \cdot \sum_{i=1}^{4} a_i e^{j\pi(4-i)\left(u+\frac{v}{2}\right)} \cdot du \cdot C \cdot \sum_{i=1}^{4} a_i e^{j\pi(4-i)\left(u+\frac{v}{2}\right)} = \sum_{i=1}^{4} b_i \cdot e^{j\pi(4-i)u} \tag{2.17}$$

Which, after working out, gives

$$8C^2 \cdot \sum_{i=1}^{4} b_i \cdot e^{j\pi(4-i)u} = \sum_{i=1}^{4} b_i \cdot e^{j\pi(4-i)u} \tag{2.18}$$

And so, if C is chosen to be $\frac{1}{\sqrt{8}}$, B is indeed an orthonormal basis for S and a normal basis for S for every other value of C ■

Consequently, once the first beam is constructed, three phase-shifted copies should be constructed. The second, third and fourth beam should be a shifted copy of the first beam by respectively $\frac{1}{2}$, 1 and $\frac{3}{2}$ in u-space.

A well-known beam basis is the set of Butler beams (Butler and Lowe 1961) shown in Figure 13, which is constructed using the beam of the linear broadside array as the first beam. The main beam (solid squares) was used to construct the other three beams. The sum of these four beams is equal to one (dashed line).

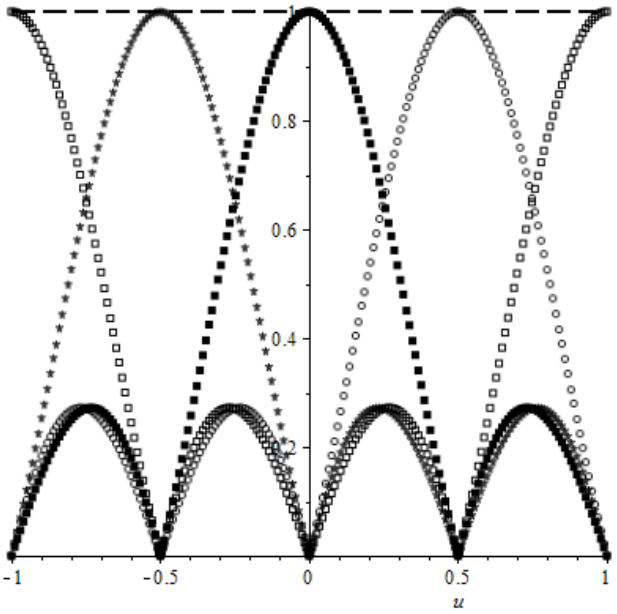

Figure 13: The butler beams form a beam basis.

And so, for every beamforming strategy, one of the beams will be determined by the strategy. Next, the other three beams are derived from this beam using the method described in this section. Then, the four orthogonal beams together will always form a basis for the function set of all phase-weighted beams. And thus, any other beam can be constructed using these four beams.

3 Two beamforming strategies

Two strategies for beamforming in the analogue frontend are investigated in this chapter. For both strategies, first the phase shifts to construct the first beam are determined. Then, the phase shifts for the other three beams immediately follow from this, using the method to create four orthogonal beams described in the previous section.

The first strategy is known as beamsteering –or– the fixed beamshape strategy. This strategy uses one fixed beamshape (shape of the radiation pattern), that of the linear broadside array antenna, that is shifted in u-space. Since the beamshape of the linear broadside array antenna is used, always an in u-space shifted set of the Butler beams is created. By shifting the set of Butler beams in u-space, the zeros of all beams, but one, can be steered towards a certain angle of incidence.

Now, using property 1 and 2 of section 1.3.4, it can be seen that this shift in u-space is achieved by applying 4 uniformly increasing phase shifts to the input signals. For example, consider a desired shift of v in u-space and an arbitrary phase shift ϕ that is applied to the first input signal. Then $\phi + v\pi, \phi + 2v\pi$ and $\phi + 3v\pi$ are the phase shifts that should be applied to the second, third and fourth input signal, respectively.

For the second strategy the constraint that the 4 phase shifts applied to the input signals should be uniformly increasing is discarded. So instead, the phase shifts applied to the first to fourth input signal are respectively ϕ, $\phi + \alpha_1\pi$, $\phi + \alpha_2\pi$ and $\phi + \alpha_3\pi$. Where ϕ, α_1, α_2 and α_3 can be chosen independent from each other. Now, the beam cannot only be shifted in u-space, but also its shape (radiation pattern) can be altered. This strategy will therefore be called the variable beamshape strategy.

In Figure 14 on the next page a graphical representation of both strategies is shown. The transparent radiation pattern behind the input lines is of the beam that would be obtained if the input signals were to be summed, no phase shifts applied. Now, note that for the fixed beamshape strategy this beam is shifted in u-space, but its shape remains the same, whereas with the variable beamshape strategy also its shape can be altered.

Note that the fixed beamshape strategy is a subset of the variable beamshape strategy where $\alpha_1 = v$, $\alpha_2 = 2v$ and $\alpha_3 = 3v$. For the remainder of this thesis the phase shift ϕ of the first input signal will be considered 0.

To be able to describe these two strategies in a concise manner, beam construction represented in matrix form is explained in the next section.

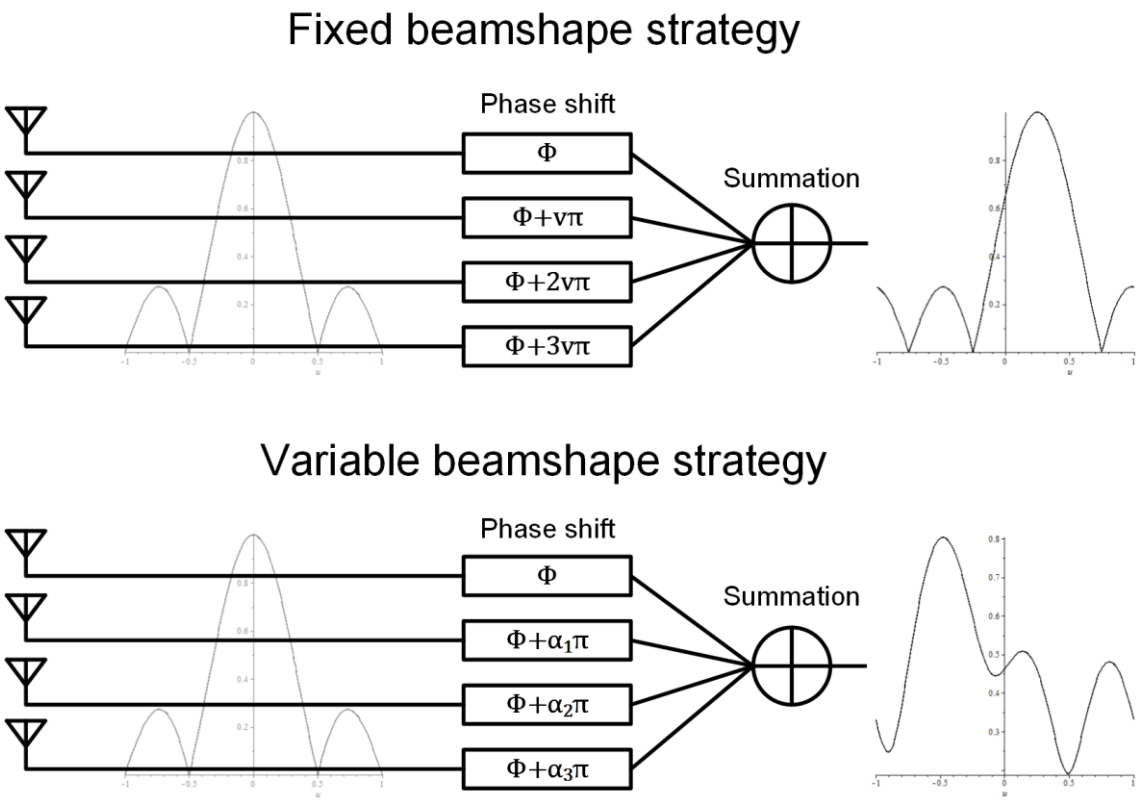

Figure 14: The fixed beamshape strategy and the variable beamshape strategy.

3.1 Beam construction in matrix form

MATLAB is a numerical computing environment that primarily excels in matrix and vector calculations. This section describes how the construction of the beams can be represented in matrix form. This representation will be used to describe both beamforming strategies. Later on this representation is also used for writing the code for the system simulation in MATLAB.

Let S be a vector of the input signals received by the elements and let A be a matrix containing the complex weights to construct the beams, then

$$T = AS \tag{3.1}$$

And for a 4-element array written out as

$$\begin{bmatrix} \mathrm{T}_1 \\ \mathrm{T}_2 \\ \mathrm{T}_3 \\ \mathrm{T}_4 \end{bmatrix} = \begin{bmatrix} a_{11} & a_{12} & a_{13} & a_{14} \\ a_{21} & a_{22} & a_{23} & a_{24} \\ a_{31} & a_{32} & a_{33} & a_{34} \\ a_{41} & a_{42} & a_{43} & a_{44} \end{bmatrix} \begin{bmatrix} S_1 \\ S_2 \\ S_3 \\ S_4 \end{bmatrix} \tag{3.2}$$

Where T is the vector consisting of the constructed beams.

Once the complex weights for the first beam are decided, so are the weights for the other beams. After all, the other beams are in u-space shifted copies of the first beam as was described in the previous section.

Furthermore, since all complex weights should have a magnitude of one, that is $|a_{ij}| = 1$, all complex weights are phase weights and thus of the following form

$$\alpha \in \mathbb{R} : e^{j\alpha} \tag{3.3}$$

Therefore, the matrix A can be split into two parts: a part, A', containing the adjustable phase weights and a part, B, containing the fixed phase weights to construct a beam basis.

That is, matrix A' is defined as

$$A' = \begin{bmatrix} e^{j\pi 0} & 0 & 0 & 0 \\ 0 & e^{j\pi\alpha_1} & 0 & 0 \\ 0 & 0 & e^{j\pi\alpha_2} & 0 \\ 0 & 0 & 0 & e^{j\pi\alpha_3} \end{bmatrix} \tag{3.4}$$

And matrix B is defined as

$$B = \begin{bmatrix} e^{j0\pi} & e^{j0\pi} & e^{j0\pi} & e^{j0\pi} \\ e^{j\frac{3}{2}\pi} & e^{j1\pi} & e^{j\frac{1}{2}\pi} & e^{j0\pi} \\ e^{j3\pi} & e^{j2\pi} & e^{j1\pi} & e^{j0\pi} \\ e^{j\frac{9}{2}\pi} & e^{j3\pi} & e^{j\frac{3}{2}\pi} & e^{j0\pi} \end{bmatrix} = \begin{bmatrix} e^{j0\pi} & e^{j0\pi} & e^{j0\pi} & e^{j0\pi} \\ e^{j\frac{3}{2}\pi} & e^{j1\pi} & e^{j\frac{1}{2}\pi} & e^{j0\pi} \\ e^{j1\pi} & e^{j0\pi} & e^{j1\pi} & e^{j0\pi} \\ e^{j\frac{1}{2}\pi} & e^{j1\pi} & e^{j\frac{3}{2}\pi} & e^{j0\pi} \end{bmatrix} \tag{3.5}$$

And now T can be calculated as

$$T = BA'S \tag{3.6}$$

3.2 The fixed beamshape strategy

To explain the fixed beamshape strategy, once again, consider the beam basis in Figure 13. Now, if an interferer originates from $u = 0$, it is completely captured in de main beam (solid squares). Since all other beams have a zero at $u = 0$, they are not affected by the interferer. And thus, discarding or attenuating the main beam would ensure proper conversion of the input signals by the ADC.

Now, consider an interferer that originates from $u = 0.2$, though. The interferer is now present in all beams. And all beams have to be discarded or attenuated to ensure proper conversion by the ADC.

The solution for this, proposed as the fixed beamshape strategy, is to shift –or– steer all beams in u-space. By *steering* the main lobe of the main beam to $u = 0.2$, the interferer would, once again, be completely captured in the main beam not affecting the other three beams. A graphical representation of the fixed beamshape strategy can be seen in Figure 15.

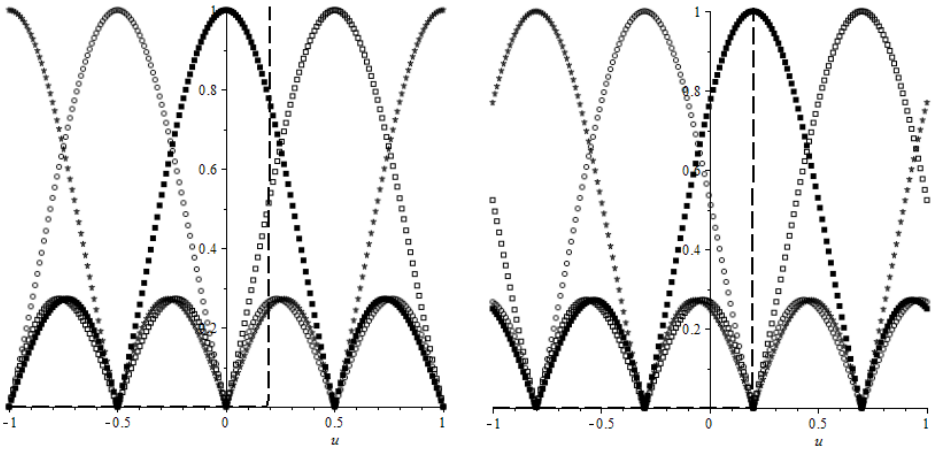

Figure 15: (left) The interferer (dashed) at u=0.2 affecting all beams (right) all beams steered by u=0.2, so the interferer only affects one beam (solid squares).

The fixed beamshape strategy can be represented in matrix form as

$$T = BA'S \tag{3.7}$$

Where B is defined as in equation 3.5 and A' is defined as below.

$$A' = \begin{bmatrix} e^{j\pi 0} & 0 & 0 & 0 \\ 0 & e^{j\pi v} & 0 & 0 \\ 0 & 0 & e^{j\pi 2v} & 0 \\ 0 & 0 & 0 & e^{j\pi 3v} \end{bmatrix} \tag{3.8}$$

Where v is the shift in u-space applied to the set of Butler Beams. This shift in u-space of v is achieved by applying a uniformly increasing phase shift to the input signals.

The phase shifters needed to apply the phase weights are easier to implement if they are quantised with a low number of bits. Therefore, different numbers of quantisation bits will be looked at in the numerical analysis.

3.3 The variable beamshape strategy

The variable beamshape strategy is identical to the fixed beamshape strategy except that it loses the constraint that the applied phase shifts have to be uniformly increasing. Therefore, radiation patterns of more different shapes can be constructed. As an example the radiation patterns of some orthogonal beam sets that can be constructed using this strategy are shown in Figure 16 on the next page.

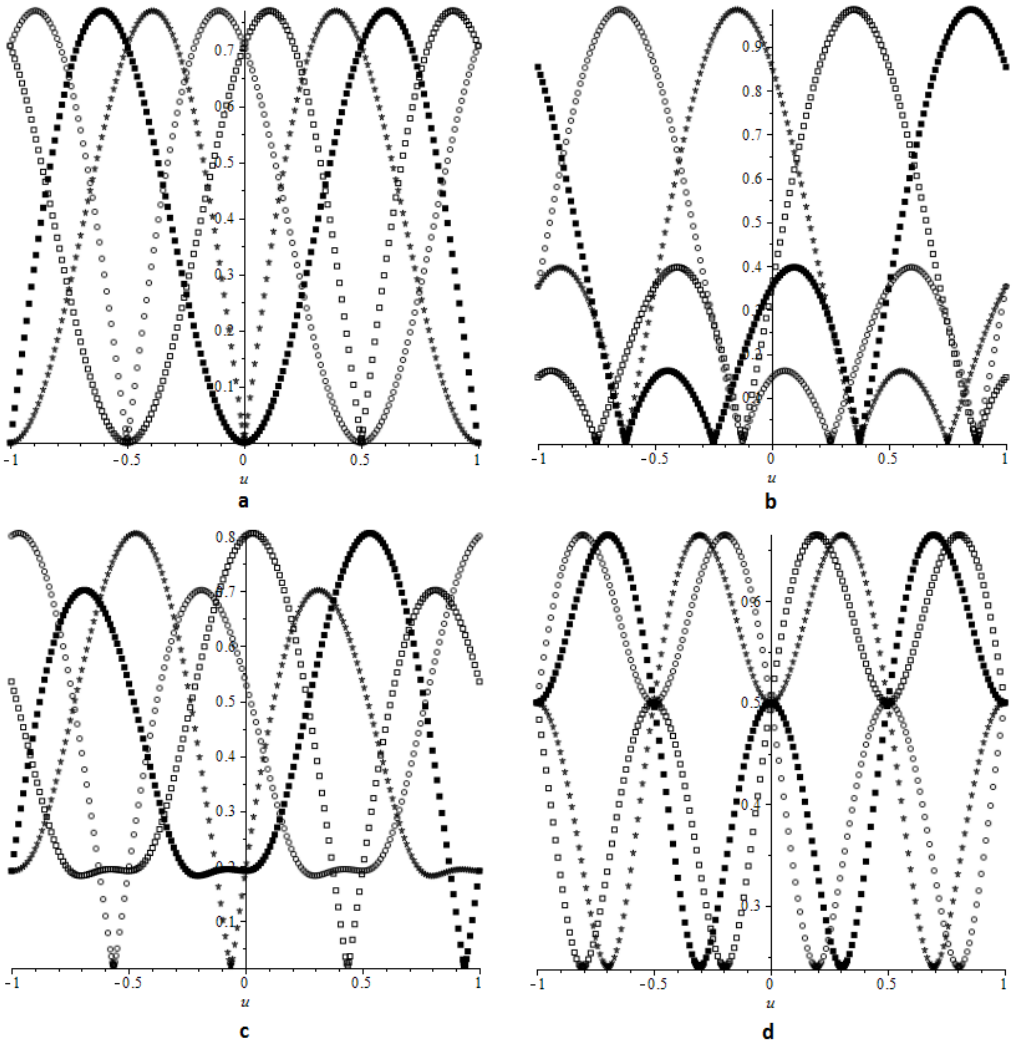

*Figure 16: Radiation pattern of some possible orthogonal beam sets constructed using the variable beamshape strategy. (**a**.* $\alpha = [0,0,1,1]$, ***b***. $\alpha = \left[0,\frac{1}{4},\frac{1}{4},\frac{1}{2}\right]$, ***c***. $\alpha = \left[0,0,1,\frac{5}{4}\right]$ ***d***. $\alpha = [0,1,1,1]$)

Once again, the phase shifters needed to apply the phase shifts of the variable beamshape strategy are quantized with a low number of bits.

For this strategy matrix A' is still defined as in equation 3.4 and the phase weights are defined as

$$\alpha_1, \alpha_2, \alpha_3 \in \left\{\alpha : n \in \mathbb{Z} \ \wedge \alpha = \frac{2 \cdot n}{2^N} \wedge n < 2^N\right\} \tag{3.9}$$

Where N is the number of bits of the quantized phase shifters.

4 Numerical analysis of the beamforming strategies

In this section a simulation method is described to compare the performances of the strategies described in the previous chapter. The simulation is conducted in MATLAB and the results are compared using the figures of merit described in the first section of this chapter.

4.1 Figures of merit

To be able to compare different strategies for beamforming some figures of merit (FOM) have to be defined. These FOMs are described in this section.

Let $P(u)$ be the normalised power radiation pattern of the array antenna after summing the constructed beams, then two figures of merit (FOM) are used to compare the two strategies

1. $P_{avg} = \int_{-1}^{1} P(u) \cdot du$
   P_{avg} is the average power received from all directions. It says something about the possibility to construct any other beam from the four orthogonal beams after AD-conversion.

2. $P_{desired} = P(u_{desired})$
   $P_{desired}$ is the power received from the direction $u_{desired}$. It says something about the possibility to receive a signal from the direction $u_{desired}$ given an interferer from any angle.

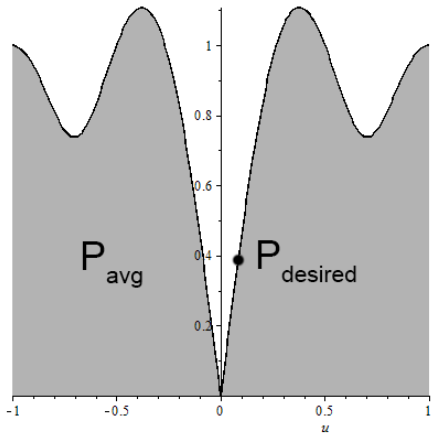

Figure 17: Graphical representation of P_{avg} and $P_{desired}$.

In figure 16 a graphical representation of P_{avg} and $P_{desired}$ is shown. Plotted in black is the sum of three of the four beams which were shown in Figure 13. The interferer is considered to be originating from $u = 0$, completely captured in the main beam. This beam is therefore discarded. The sum of the remaining three beams after normalisation is the normalised power radiation pattern plotted in black.

Now, P_{avg} is the area in grey under the plot and, $P_{desired}$ is the value of the normalized power radiation pattern at $u = 0.1$, assuming $u_{desired} = 0.1$.

4.2 Simulation method

For both strategies all possible orthogonal beam sets are constructed, while considering some interferer at the input of the system. Next, all the beams are examined and the beams whose magnitude exceed the voltage range of the ADC are discarded. Hereafter the radiation pattern of the beam set is determined by summing the remaining beams and the FOMs of the pattern are calculated.

This process is repeated for all possible angles of incidence of the interferer. Next, for both strategies, the beam set with the best result for a certain interferer and FOM is selected. Then, the two strategies can be compared for all interferers for both FOMs.

Alongside the number of bits of the phase shifters of both strategies, also the magnitude of the interferer will be varied between simulations. The magnitude of the interferer is normalised with respect to the voltage range of the ADC after amplification by the RF frontend and therefore expressed in dBFS. That is, an interferer with a magnitude of 0 dBFS signifies an interferer whose magnitude equals the ADC's voltage range after amplification by the RF frontend. The different values of the parameters that will be simulated can be seen in Table 1.

Table 1: Values of the parameters varied between simulations of the system.

Parameter	Values
Resolution of the phase shifters of the fixed beamshape strategy	2, 3 and 4 bits
Resolution of the phase shifters of the variable beamshape strategy	2, 3 and 4 bits
Magnitude of the interferer	6, 14 and 20 dBFS

The MATLAB code performing the simulations can be found in Appendix A. The results of the simulations are discussed in the next section.

4.1 Simulation results

The results of the simulations described in the previous section are displayed in 6 different figures. Each figure contains the results of one of the two strategies for one of the simulated interferer magnitudes. Every figure contains six plots. That is, both FOMs times the simulated number of resolutions of the phase shifters.

Every plot shows the value of the FOM in dB against the angle of incidence of the interferer in u-space. For $P_{desired}$ is considered $u_{desired} = 0$.

The plots for the fixed beamshape strategy for an interferer magnitude of 6, 14 and 20 dBFS can be seen in respectively figure Figure 18, Figure 19 and Figure 20.

The plots for the variable beamshape strategy for an interferer magnitude of 6, 14 and 20 dBFS can be seen in respectively figure Figure 21, Figure 22 and Figure 23.

As discussed in the previous section, a beam whose magnitude falls outside of the range of the ADC is regarded as lost and completely discarded before calculating the performance measures. That is why a lot of sudden jumps (discontinuities) can be seen in the graphs of P_{avg}. Empty parts in the graphs represent the value 0 (-∞ dB).

For both strategies, a higher value for a figure of merit for a certain angle of incidence of the interferer means better performance. Empty parts in the plots represent the value 0 and mean that the receiver is completely desensitized.

Looking at the results of the simulation the following observations can be made.

1. The variable beamshape strategy clearly outperforms the beamsteering strategy when both strategies use the same phase shifter resolution. For similar performance beamsteering requires a 2 bit higher phase shifter resolution.
2. No performance is gained by increasing the phase shifter resolution of the variable beamshape strategy above 2 bits for interferer magnitudes of 6 dBFS and lower.
3. No performance is gained by increasing the phase shifter resolution of the variable beamshape strategy above 3 bits for interferer magnitudes of 14 dBFS and lower.

From these observations the next two conclusions can be drawn.

1. For the same resolution the fixed beamshape strategy is clearly outperformed by the variable beamshape strategy. Both strategies can be implemented in a similar fashion: fixed phase shifters to obtain the Butler Beams followed by four phase shifters to apply the per element phase shift. Therefore, unless if somehow the uniformly increasing phase shifters can be exploited to reduce the implementation cost, the variable beamshape strategy is the better choice of the two strategies.
2. A higher phase shifter resolution increases performance for higher interferer magnitudes, but is also more difficult to implement.

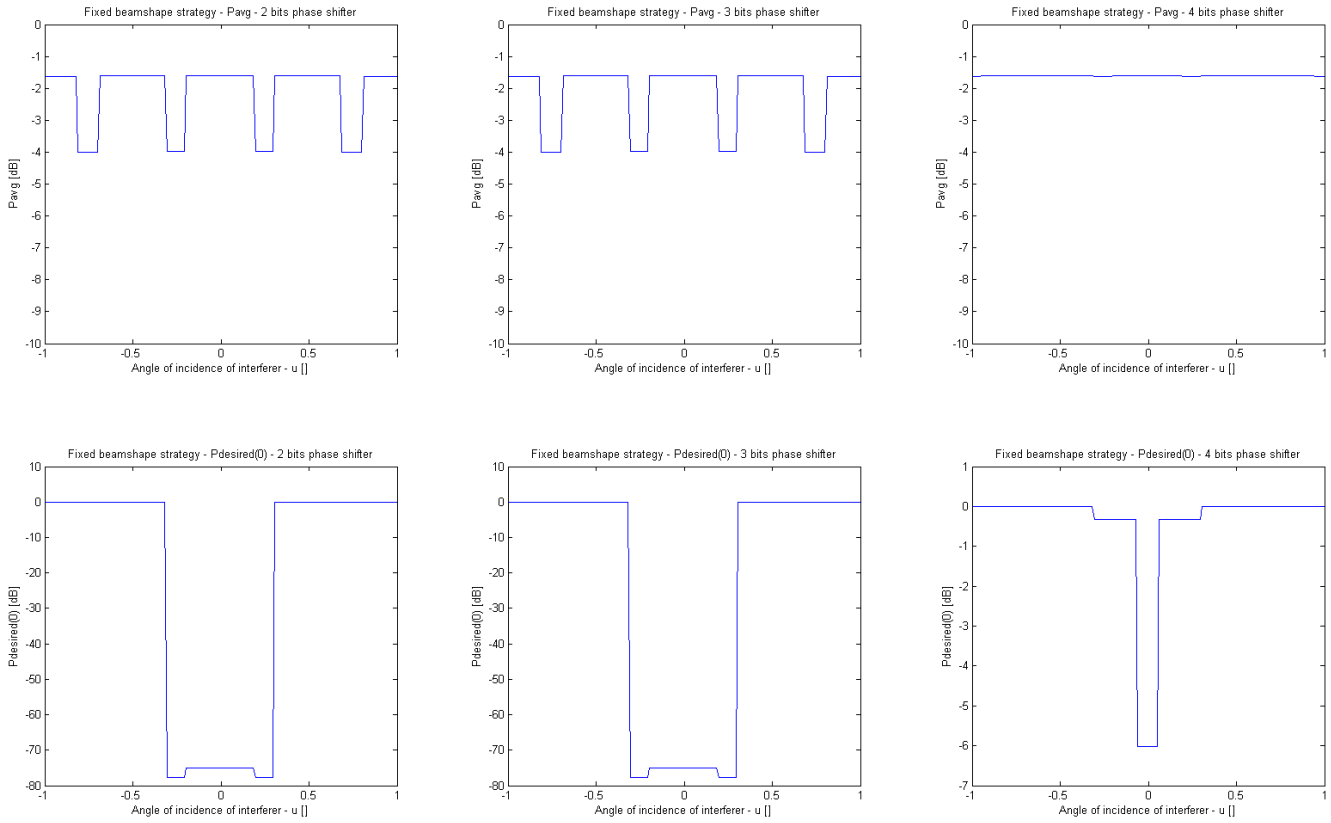

Figure 18: Figure of merits fixed beamshape strategy for an interferer of 6 dBFS.

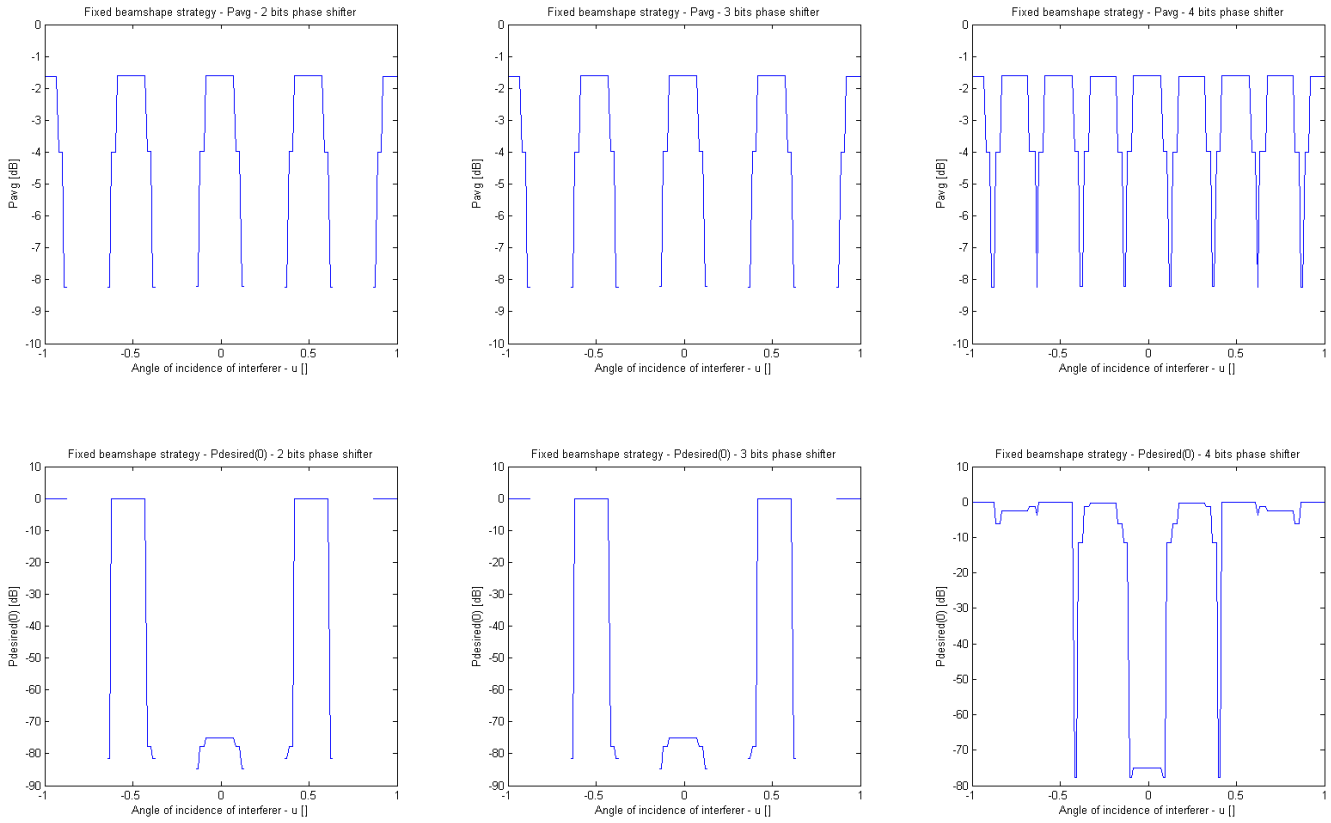

Figure 19: Figure of merits fixed beamshape strategy for an interferer of 14 dBFS.

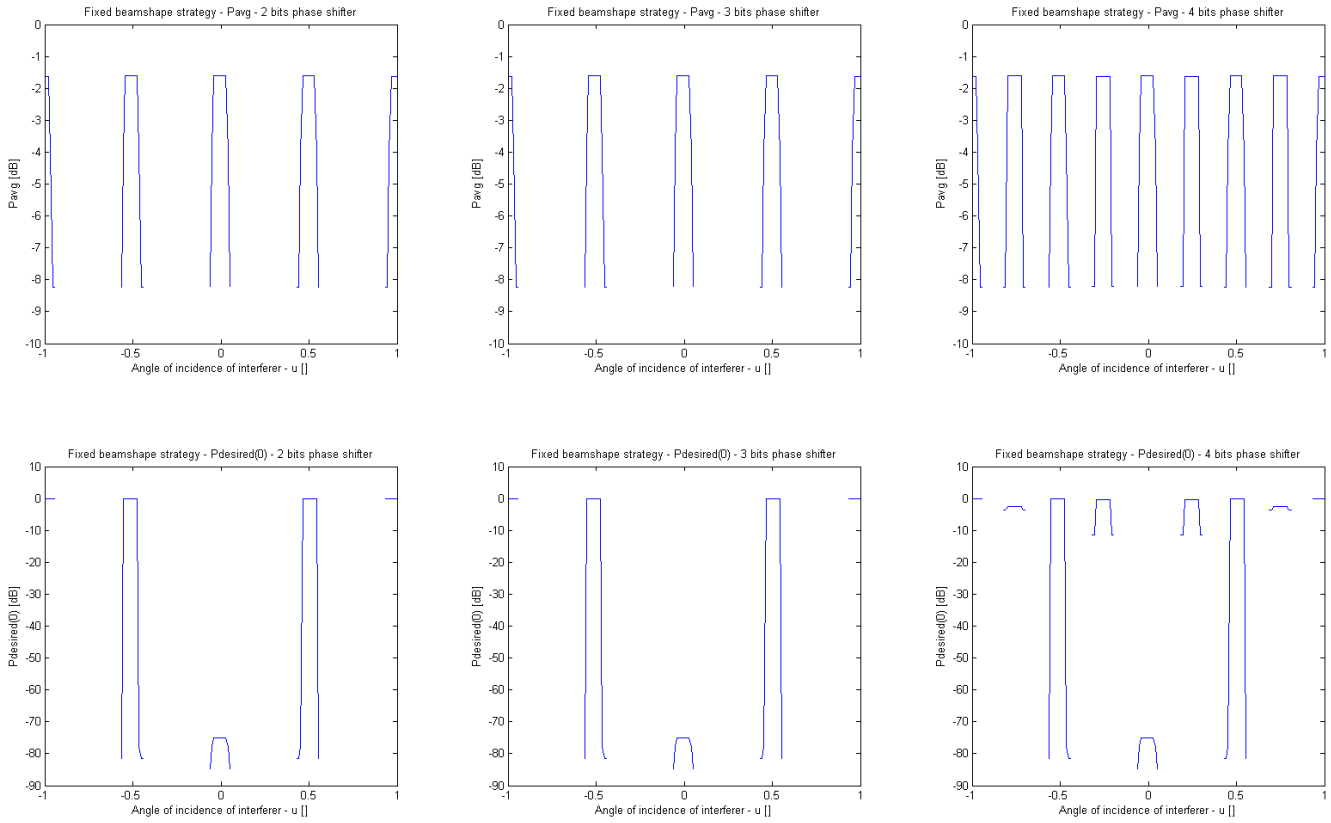

Figure 20: Figure of merits fixed beamshape strategy for an interferer of 20 dBFS.

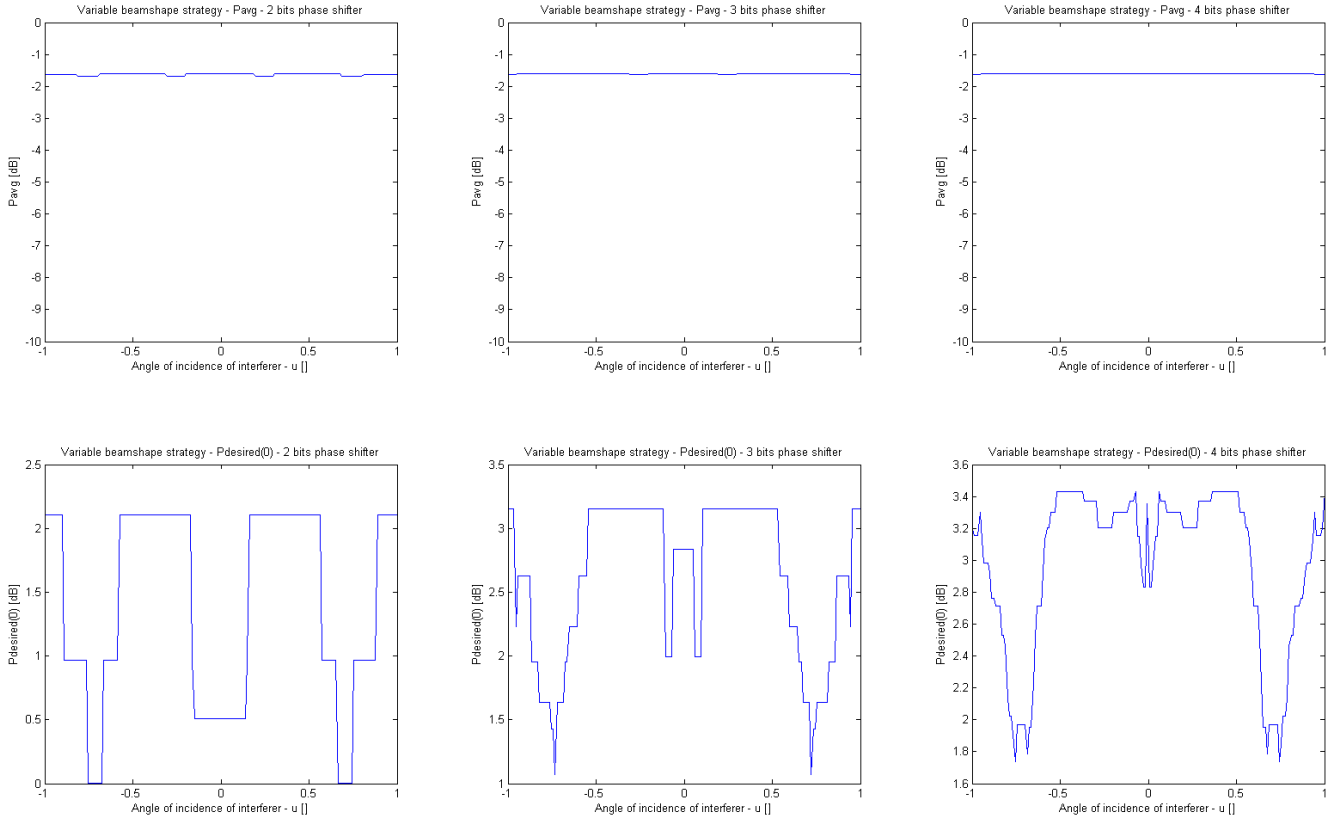

Figure 21: Figure of merits variable beamshape strategy for an interferer of 6 dBFS.

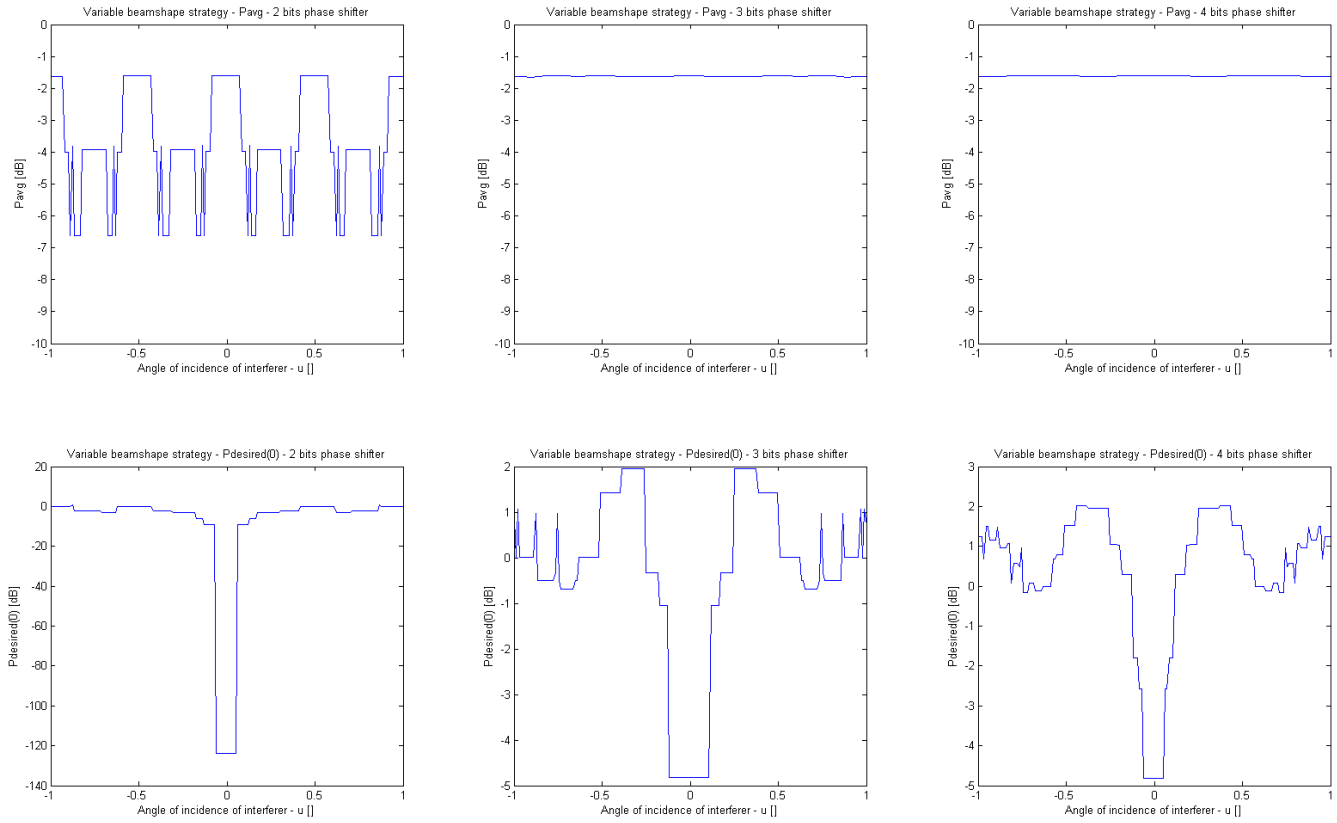

Figure 22: Figure of merits variable beamshape strategy for an interferer of 14 dBFS.

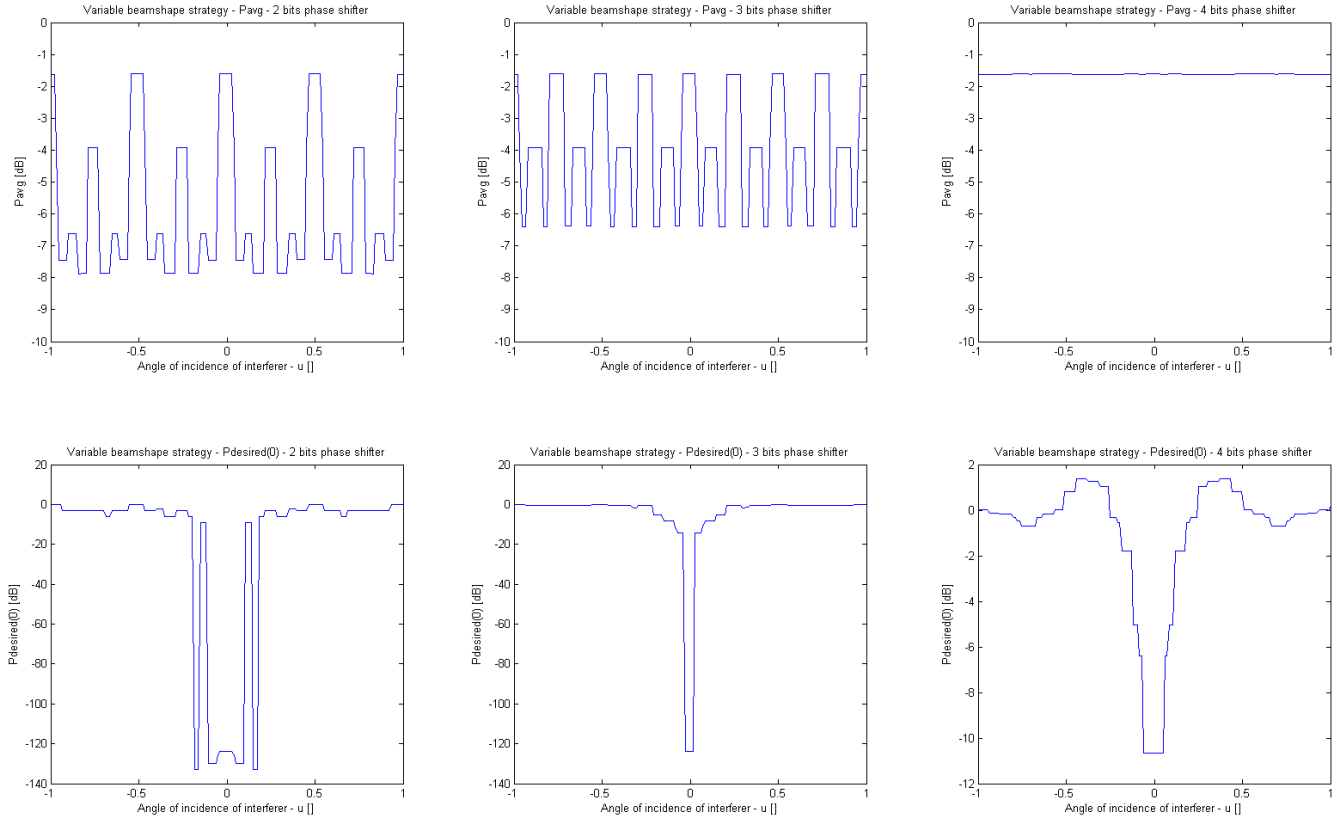

Figure 23: Figure of merits variable beamshape strategy for an interferer of 20 dBFS.

4.2 System choices and specifications

In this chapter two beamforming strategies have been discussed that can be implemented to improve the performance of the system under influence of a strong interferer. One of the two strategies uses a fixed beamshape that is shifted in u-space. The other strategy uses a variable beamshape. In the previous section it is showed that the ability to use differently shaped beams is beneficial for beamforming and the variable beamforming strategy is therefore the preferred choice for beamforming.

In this section first the implementation of the variable beamshape strategy is discussed. In the subsequent section specifications for the circuit design implementing this strategy are motivated.

4.2.1 Implementation of the variable beamshape strategy

In the previous section an implementation of beamforming using a fixed phase-shifting network and 4 variable phase shifters was briefly discussed. It is also possible to implement beamforming using the 8 already for harmonic rejection available LO phases.

Then, beamforming can be implemented by *routing* the LO phase shifter outputs to 4 summators. This routing logic can be implemented by a multiplexer that routes each LO phase shifter output to one of the 4 summators. Now, not only the phase shift of all input signals of one element can be adjusted together, but also the phase shift of each individual input signal can be adjusted. Therefore, this implementation not only saves 4 phase shifters, but also the fixed phase-shifting network to construct the Butler Beams is not needed anymore.

Since, 8 LO phases are available this thesis explores to implement the variable beamshape strategy with 3 bit (8) phase shifters. Therefore, in theory, interferers up to 14 dBFS can be captured in one beam without affecting the performance of the frontend.

4.2.2 Specifications of the mixer

The main goal of the frontend in this work is to achieve a higher performance under influence of an interferer, than a frontend not implementing beamforming would. The performance gained by implementing beamforming can be expressed by an increase of the 1dB desensitisation point as well as an increase of the signal-to-interferer ratio (SIR).

The 1dB desensitisation point is the input power level of the interferer that causes a 1dB drop in the linear gain of the wanted signal. Implementing beamforming should make the receiver more robust against strong interferers. And, as such, the 1dB desensitisation point should shift to higher power levels of the interferer, as is shown in Figure 24.

The SIR of a system is defined as the power ratio from the wanted signal to the interferer at the output of the system.

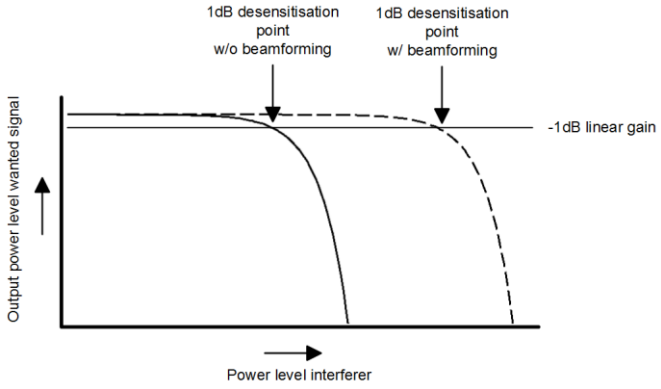

Figure 24: The 1dB desensitisation point.

The implementation of beamforming in the mixer should not affect other properties of the mixer like noise performance and linearity (too much). In (Shen 2011) the specifications of down-conversion mixers in both CMOS and BiCMOS of some other works can be found. These specifications are shown in Table 2 and are used as a reference point for the implementation of the mixer implementing beamforming.

Table 2: Specifications of down-conversion mixers of other works.

SPECIFICATION	VALUE
NOISE FIGURE	12..20 dB
IIP3	1..10 dBm
1-DB COMPRESSION POINT	-6..2 dBm
GAIN	12..16 dB
POWER CONSUMPTION	3..18 mW

5 Circuit level design implementing beamforming

In this chapter the circuit level implementation of the variable beamshape beamforming strategy is discussed. The circuit is implemented using the QUBiC4Xi BiCMOS process of NXP. Phase-shifted versions of the input signal created by duplicating the mixer for multiple LO phases: the LO phase shifters, are used to implement beamforming. Then, for each beam 4 (one of each element) of these phase-shifted signals have to be summed.

So, first, for each element of the antenna array 8 phase-shifted copies of the input signal are created, using the 8 LO phases. Then all these phase-shifted signals are fed to a multiplexer, which then routes these signals to 8 summators. After summation 4 differential beams have been created. An overview of this implementation in building blocks can be seen in Figure 25.

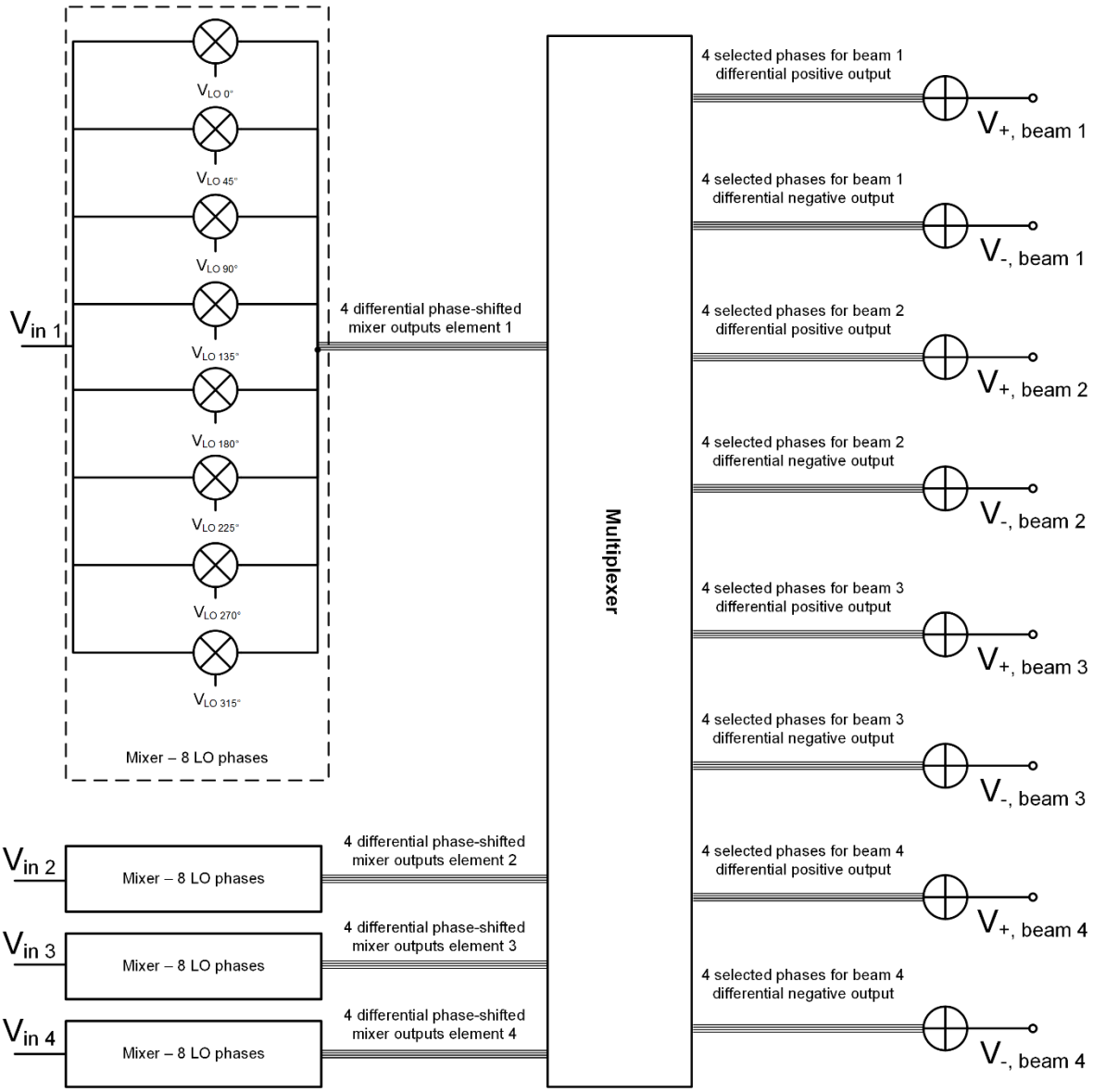

Figure 25: Block diagram of the circuit level design implementing beamforming.

5.1 Efficient beam construction

For the block diagram in figure 21 it was assumed that each LO phase shifter output would only be used once. For the current beam construction strategy this is not necessarily true, though. This section describes a slight adjustment to the beamforming matrix B of equation 3.5 so that every phase-shifted mixer output is only used once.

Then, if the mixer would provide a differential output, only four mixers would have to be implemented to obtain the 8 phase-shifted versions of the input signal needed for beamforming. For these 4 mixers to be sufficient to create all beams two conditions have to be met:

1. Every phase-shifted version of an element's signal can only be used once to ensure equal load on all mixers. For example, if the 45° phase-shifted signal of the first element is used to create the first beam, this signal cannot be used anymore to create any of the other three beams.
2. Since all beams are created as differential signals, if one output of the mixer is used to create a beam the complementary output of the mixer also cannot be used anymore to create any of the other three beams. For example, if the 45° phase-shifted signal of the first element is used to create the first beam, also the 225° phase-shifted signal of the first element cannot be used anymore to create any of the other three beams.

The matrix B from equation 3.5 used to construct the four beams does not meet these requirements. This matrix can easily be adjusted using the first property of section 1.3.4 to comply to these requirements, though. That is, the values in each column should be unique and none of the values should be the complex conjugate of each other.

Now, multiplying matrix B, by matrix Q in equation 5.1, matrix B' in equation 5.2 is obtained. This matrix B' constructs 4 beams with the same radiation patterns as those created by matrix B from equation 3.5, but does comply with the two requirements depicted in this section.

$$Q = \begin{bmatrix} e^{j0\pi} & 0 & 0 & 0 \\ 0 & e^{j\frac{1}{4}\pi} & 0 & 0 \\ 0 & 0 & e^{j\frac{1}{2}\pi} & 0 \\ 0 & 0 & 0 & e^{j\frac{3}{4}\pi} \end{bmatrix} \tag{5.1}$$

$$B' = QB = \begin{bmatrix} e^{j0\pi} & e^{j0\pi} & e^{j0\pi} & e^{j0\pi} \\ e^{j\frac{7}{4}\pi} & e^{j\frac{5}{4}\pi} & e^{j\frac{3}{4}\pi} & e^{j\frac{1}{4}\pi} \\ e^{j\frac{3}{2}\pi} & e^{j\frac{1}{2}\pi} & e^{j\frac{3}{2}\pi} & e^{j\frac{1}{2}\pi} \\ e^{j\frac{5}{4}\pi} & e^{j\frac{7}{4}\pi} & e^{j\frac{1}{4}\pi} & e^{j\frac{3}{4}\pi} \end{bmatrix} \tag{5.2}$$

5.2 The mixer

The double balanced Gilbert cell mixer (Gilbert 1968) is a favoured topology for a bipolar active mixer in RFIC design (Sulivan 1997). The Gilbert cell mixer, shown in Figure 26, is used as a starting point for the design of the mixer.

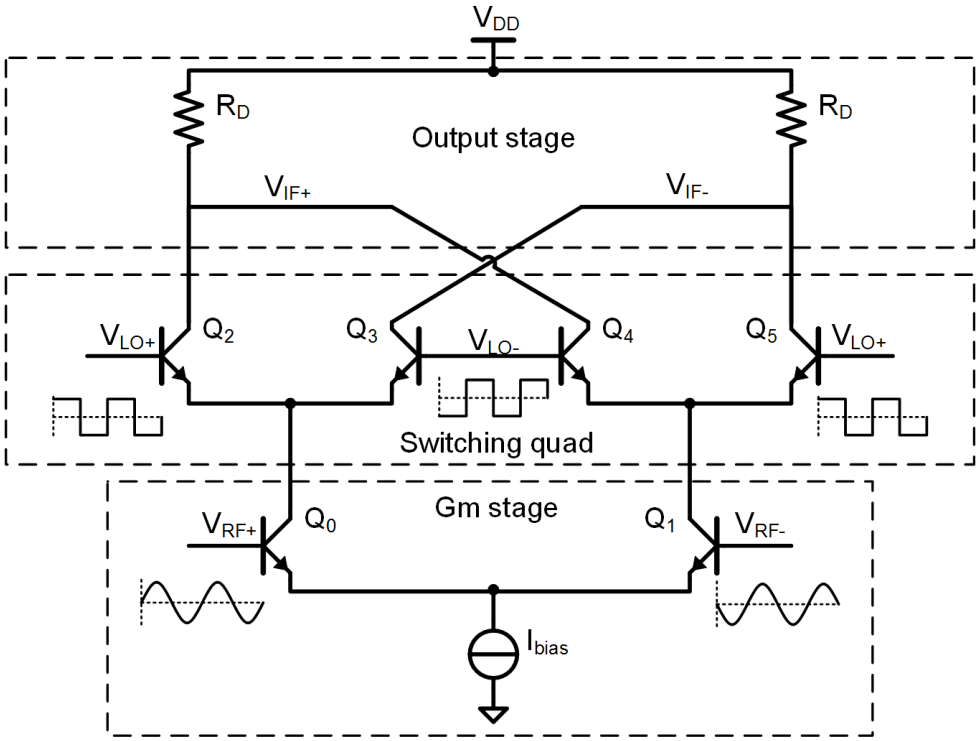

Figure 26: A Gilbert cell mixer.

The mixer has a differential RF input as well as a differential LO input and is therefore called double balanced. The RF input signal, V_{RF}, is first amplified and converted to a current by the Gm stage. The Gm stage consists of a differential pair (Q_0 and Q_1) and a current sink providing a bias current.

The four cross-coupled transistors Q_2, Q_3, Q_4 and Q_5 function as switches and together make up the switching quad. The switching quad switches the polarity of the current from the Gm stage to the output stage with V_{LO}.

Finally, a current to voltage conversion is performed by 2 resistors in the output stage to obtain the differential output voltage V_{IF}.

The design of the mixer forces compromises between conversion gain, linearity, noise and power consumption. The aforementioned mixer properties are discussed in the next subsections.

5.2.1 Noise

The noise of the mixer, assuming gain >> 1, is predominantly determined by the noise of the Gm stage. The noise of the Gm stage is for the most part built up from shot noise and base resistor noise of the both transistors and thermal noise of the degeneration resistors.

The shot noise of the transistors is observed by a shot noise current from the collector to the emitter of both transistors and is given by

$$\overline{\imath_c^2} = 2qI_C \tag{5.3}$$

Where q is the elementary charge and I_C is the collector current of the transistor. The only way to reduce the impact of the noise of these transistors is to increase the collector current. This can be seen by looking at the transconductance of a bipolar transistor which is given by

$$g_m = \frac{I_C}{V_T} \tag{5.4}$$

Where $V_T = \frac{kT}{q}$ is the thermal voltage, k is Boltzmann's constant and T is the transistor's absolute temperature. Now, since the signal power is proportional with g_m^2 and the noise power is proportional with $\overline{\imath_C^2}$, the SNR is proportional with I_C. Thus, doubling the collector bias current also doubles the SNR of the mixer.

The noise of the resistors is given by

$$\overline{v_n^2} = 4kTR \tag{5.5}$$

Where T is the resistor's absolute temperature and R is the resistor value. This voltage noise by the resistors is present at the emitter of the transistors and therefore amplified. This makes it an important noise source. The noise of the resistors can be reduced by reducing the resistor value.

The transistor base resistor is a physical resistor and therefore has thermal noise, which is given by

$$\overline{v_n^2} = 4kTr_b \tag{5.6}$$

Where r_b is base resistor value of the transistor. This resistor, and thus its noise, can be reduced by increasing the size of the transistor at the expense of the unity-gain bandwidth f_T.

5.2.2 Linearity

Linearity is basically the dependence of the gain of a circuit upon the input level. Linearization of a circuit is the principle to decrease this dependence. The simplest technique to increase the linearity of the mixer is emitter degeneration as is shown in Figure 27.

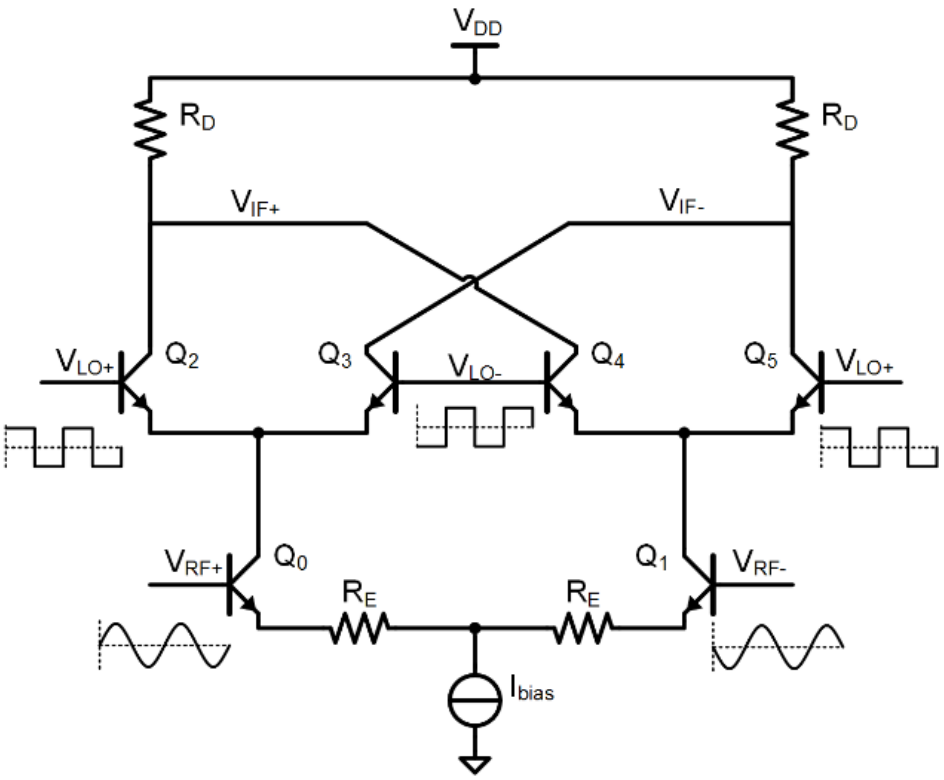

Figure 27: Gilbert mixer with resistive emitter degeneration.

The equivalent transconductance of the Gm stage, when degenerated with resistors is given by

$$G_m = \frac{g_m}{1+g_m R_E} \tag{5.7}$$

This transconductance approaches $\frac{1}{R_E}$ for large values of $g_m R_E$, a value that is independent of the input level of the mixer.

Emitter degeneration can also be implemented using inductors. An advantage of using inductors is the better noise performance of inductors in comparison with resistors. This comes at the cost of a (much) larger needed chip area, though.

Better linearity can be obtained by increasing R_E, this comes at the cost of a higher noise figure, though.

5.2.3 Conversion gain

The output voltage of the mixer is given by:

$$v_{IF} = \frac{2}{\pi} \cdot v_{RF} \cdot G_m \cdot R_D \tag{5.8}$$

Where G_m is the transconductance of the Gm stage. The factor $\frac{2}{\pi}$ appears in the equation, because a square wave instead of a sine is used to switch the switching quad.

The conversion gain of the mixer is then determined by the ratio of the load resistance and the degeneration resistance and given by

$$CG = \frac{v_{IF}}{v_{RF}} = \frac{2}{\pi} \cdot \frac{g_m R_D}{g_m R_E + 1} \approx \frac{2}{\pi} \cdot \frac{R_D}{R_E} \quad (if\ g_m R_E \gg 1) \tag{5.9}$$

So, to increase the conversion gain of the mixer either the value of R_D can be increased or the value of R_E can be reduced.

5.2.4 Power consumption

The power consumption of the mixer is completely determined by the current of the current sink. This current is in its turn determined by the value of R_D and the current injected at the collector of Q_0 and Q_1. The current of the current sink has to be such that the output signal can achieve maximum swing. The supply voltage minus the headroom voltage of the stacked transistors and the current sink is the total headroom available to the output signal. Now I_{bias} should be such that the dc voltage drop over R_D is half of that. That is,

$$I_{bias} = \frac{V_{DD} - V_{stack}}{R_D} \tag{5.10}$$

Where V_{stack} is the minimum headroom voltage needed for the stacked transistors and current sink.

The total current consumption of the circuit is then the current of the sink plus some overhead current to create the reference current for the current mirror and the bias voltages.

$$I_{total} = I_{bias} + I_{overhead} \tag{5.11}$$

The current consumption times the power supply is the power consumption of the mixer. That is,

$$P = V_{DD} \cdot \left(\frac{V_{DD} - V_{stack}}{R_D} + I_{overhead} \right) \tag{5.12}$$

The power consumption of the mixer can be reduced by either increasing R_D or decreasing the supply voltage.

5.2.5 Current sink

The current sink is implemented by a current mirror. The circuit of a current mirror is shown in Figure 28.

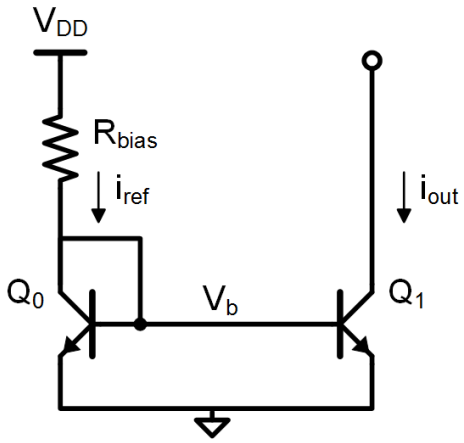

Figure 28: A bipolar current mirror.

The reference current of the current mirror is given by

$$I_{ref} = \frac{V_{DD} - V_b}{R_{bias}} \tag{5.13}$$

The output current of the mirror is equal to the reference current minus the base currents of Q_0 and Q_1. Thus, the output current of the mirror is then related to the reference current by

$$I_{out} = \frac{n \cdot i_{ref}}{1 + \frac{1+n}{\beta_{F0}}} \tag{5.14}$$

Where β_{F0} is the forward common emitter current gain of the transistors for $V_{CB} = 0$ and n is the ratio of the emitter areas of Q_0 and Q_1. Now, by making Q_0 much smaller than Q_1 and moreover reusing the reference current for multiple mixers, the overhead current consumption of the current sink becomes negligible.

The voltage at the collector of Q_1 may be higher than V_b and thus $V_{CB} > 0$ for Q_1. Hence, the Early effect would occur, affecting the base current of Q_1 and therewith i_{out}. The matching of the reference current and the output current of the current mirror is not important for its function as current sink, though. Therefore the Early effect is neglected.

5.2.6 Harmonic rejection

Harmonic rejection can be implemented by splitting the mixer into three mixers. The output signals of these mixers then can be summed by connecting them after the switching quad, but before the output stage, which is implemented only once. The output currents of the mixers are summed according to Kirchoff's current law.

The emitter area of the transistors, the degeneration resistors and the current of the current sink then have to be scaled to achieve the same mixer properties as the mixer before splitting. By scaling the three mixers in a ratio of 5:7:5 and switching them with respectively LO_{-45°, LO_{0° and LO_{+45° harmonic rejection can be achieved. The resulting circuit is show in Figure 29 on the next page.

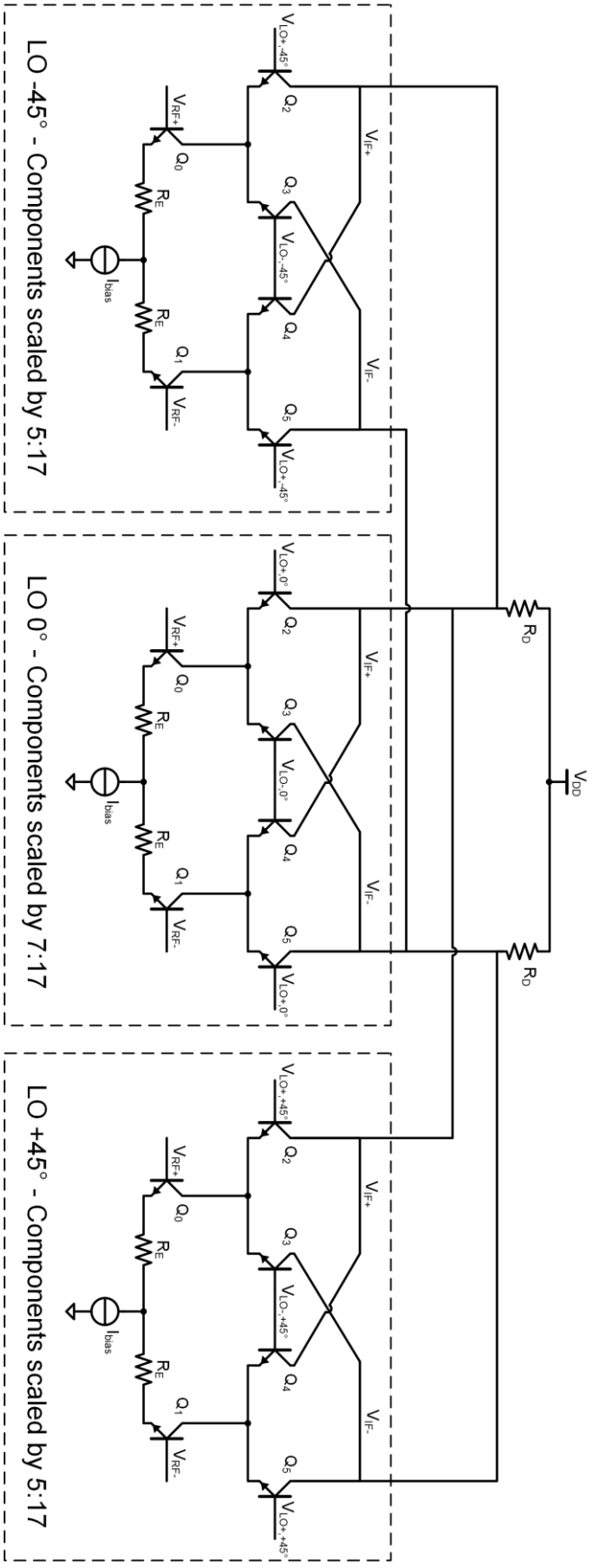

Figure 29: Implementation of harmonic rejection.

5.3 Multiplexer and summator

Now, the multiplexer can be implemented by replacing the output stage of all mixers by the circuit shown Figure 30. The circuit shows 8 MOS transistors functioning as switches to *route* the output current of the mixer to one of the four beams.

The switches are controlled by 8 control voltages (V_{1+}, V_{1-}, V_{2+}, …, V_{4-}). These 8 control voltages turn on one of the switches, while turning off the rest. For example, turning on the switches controlled by V_{1+}, will route the output current of the mixer to the summator that creates the first beam. Turning on the switches controlled by V_{1-}, will once again route the output current to the summator that creates the first beam, but this time with reversed polarity. By reversing the polarity, the output current of the mixer phase shifted by the phase shift of V_{LO-} is achieved.

The output stage of the four beams is only implemented once, while the multiplexer stage is implemented for every mixer. The 8 outputs of the multiplexer stage of all the mixers are connected to the 8 inputs of the one output stage. Then, as with harmonic rejection, the output currents of the mixers are summed according to Kirchoff's current law.

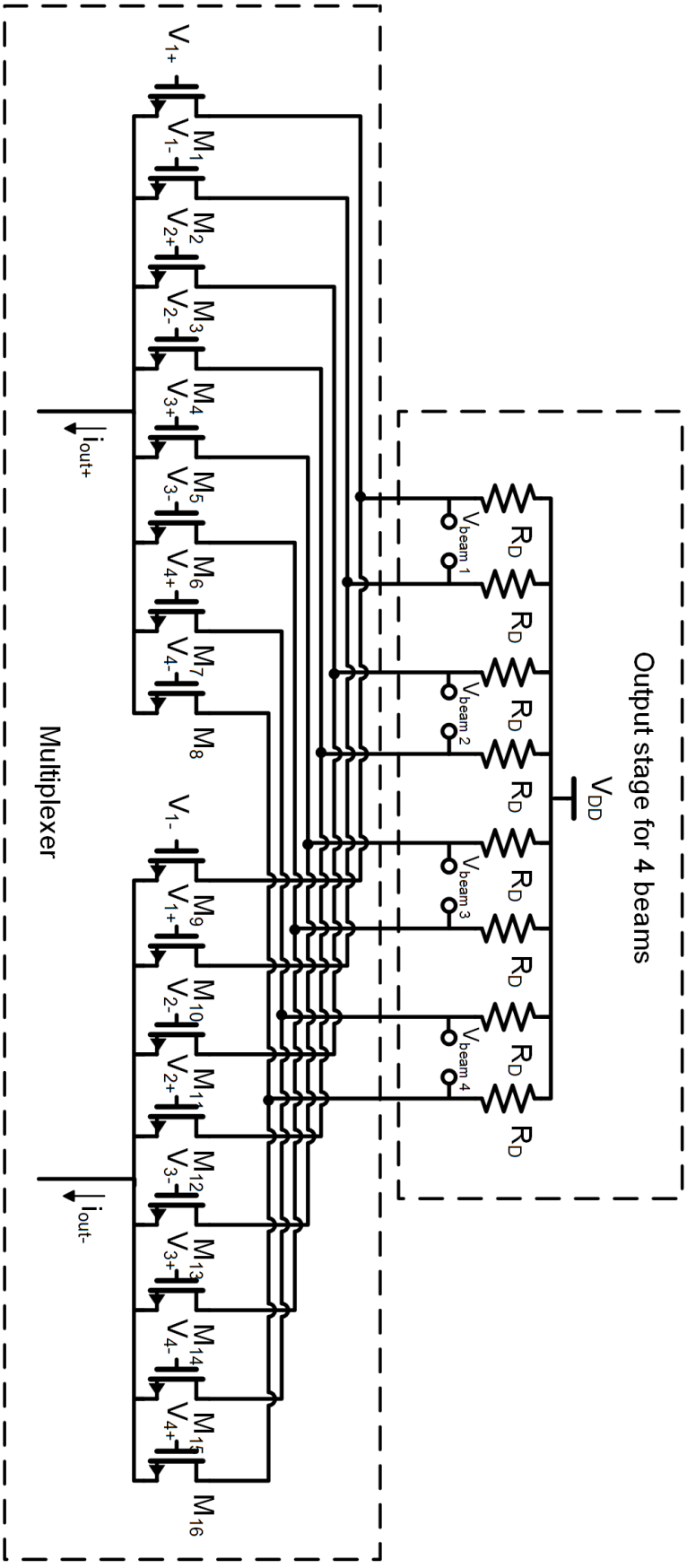

Figure 30: Gilbert cell mixer output stage implementing a multiplexer.

5.4 Overview

In Figure 31 on the next page is the implementation of the HR mixer with multiplexer shown. In the top left corner is the symbol shown that will be used to denote the HR mixer with multiplexer in the complete system overview. All the input and output signals of the mixer are differential.

In figure 32 a complete overview of the system is shown. A group of 4 mixers creating the 8 phase-shifted copies of and RF input signal will be called a phase-shifter block. Furthermore a shorthand notation is used to denote the signals of the system. For example,

$$i_{out[1..4,5..8]} = \begin{bmatrix} i_{out[1,5]} & i_{out[1,6]} & i_{out[1,7]} & i_{out[1,8]} \\ i_{out[2,5]} & i_{out[2,6]} & i_{out[2,7]} & i_{out[2,8]} \\ i_{out[3,5]} & i_{out[3,6]} & i_{out[3,7]} & i_{out[3,8]} \\ i_{out[4,5]} & i_{out[4,6]} & i_{out[4,7]} & i_{out[4,8]} \end{bmatrix}$$

In the next chapter first the performance of the phase-shifter block is discussed, followed by the beamforming performance of the complete system.

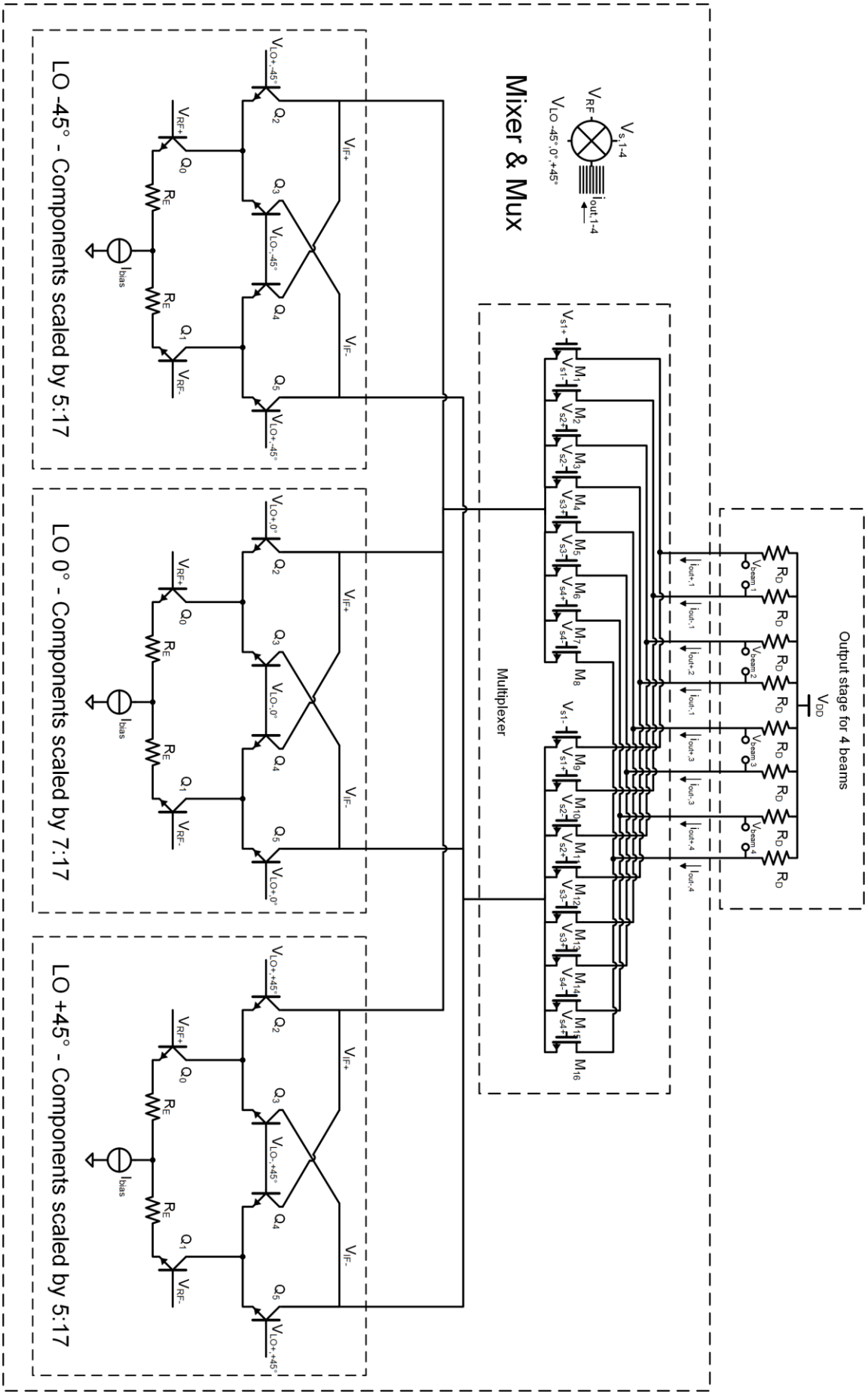

Figure 31: Implementation of the harmonic rejection mixer (LO phase shifter) with multiplexer.

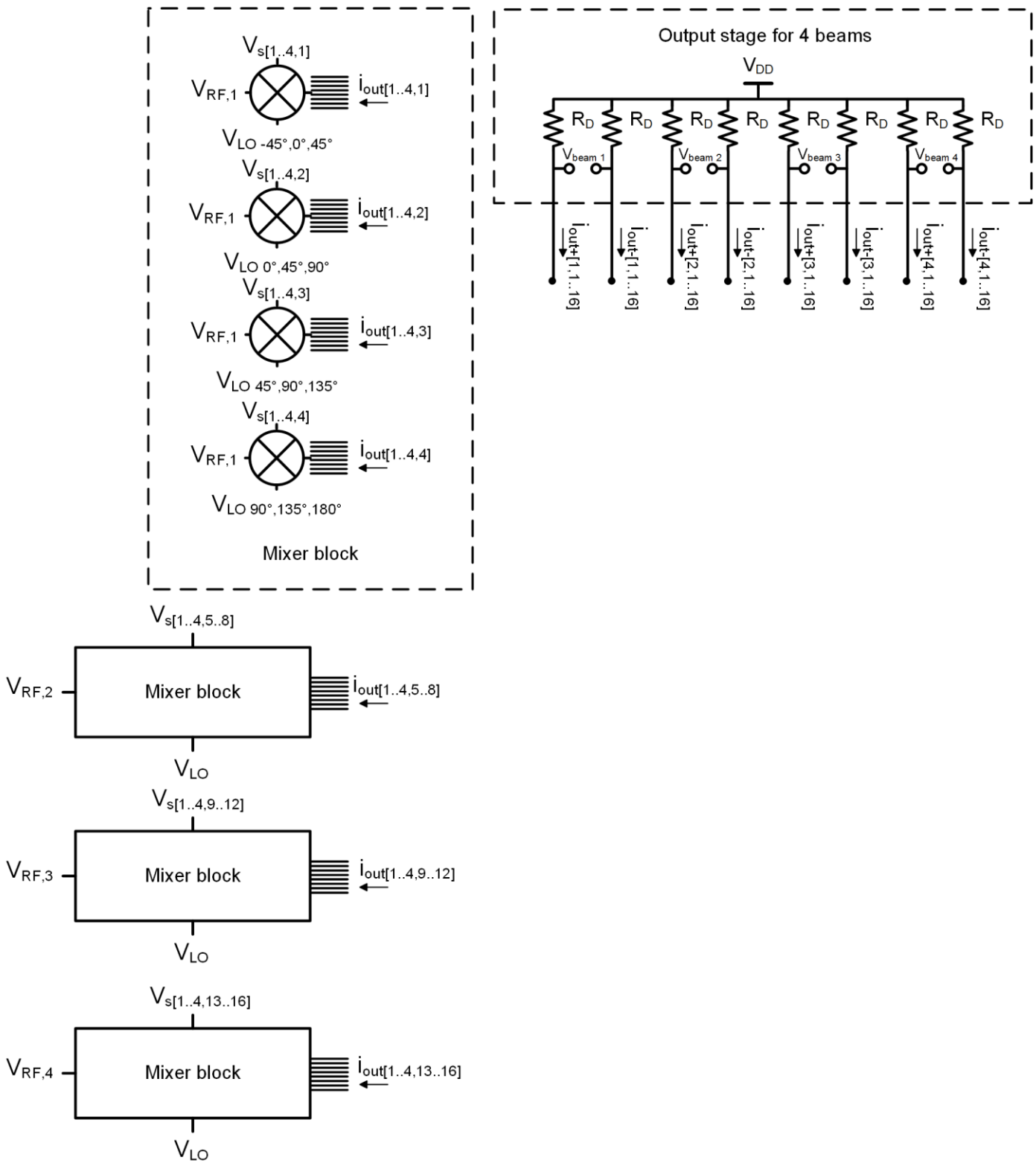

Figure 32: Overview of the implementation of the complete system.

6 Circuit level design simulation and performance

In this chapter the performance of the circuit level design proposed in the previous chapter is verified using SpectreRF simulator from Cadence design systems.

Unless stated otherwise the values for the design variables shown in Table 3 are used. The design variable gm is defined as

$$gm = \frac{R_D}{R_E}$$

Table 3: Design variables used for circuit level design simulations.

Supply voltage	5V
LO frequency	2.5GHz
LO magnitude	200mV
RF frequency	2.6GHz
R_D	600Ω
gm	20mS

The RF signals are created by ports with an internal resistance of 50Ω. A resistor of 50Ω is connected to the output of the port as a replacement for an impedance matching circuit.

The LO signals are created by ideal square wave generators. The rise and fall time of the square waves are set to 5% of the period time. Furthermore, the type of the rising and falling edge is set to halfsine for better convergence.

The bias voltages of the Gilbert cells are shown in table 4 below.

Table 4: Bias voltages for the Gilbert cells.

LO DC Bias	2.3V
RF DC Bias	1.7V

The properties of the bipolar transistors used to implement the Gilbert cells (Q_0-Q_5) are shown in Table 5.

Table 5: Properties bipolar transistors used to implement the Gilbert Cell.

Width	0.4 µm
Length	5 µm
Number of emitters	2

The properties of the NMOS transistors used to implement the multiplexer are shown in Table 6.

Table 6: The properties of the NMOS transistors used to implement the multiplexer.

Width	2 µm
Length	0.25 µm

First, the performance of a single phase shifter block is verified. Then the performance of the system implementing beamforming is compared to the same system not implementing beamforming, while both systems are subjected to an interferer.

6.1 Conversion Gain

In Figure 33 the conversion gain of the phase shifter block as a function of the variable gm can be seen.

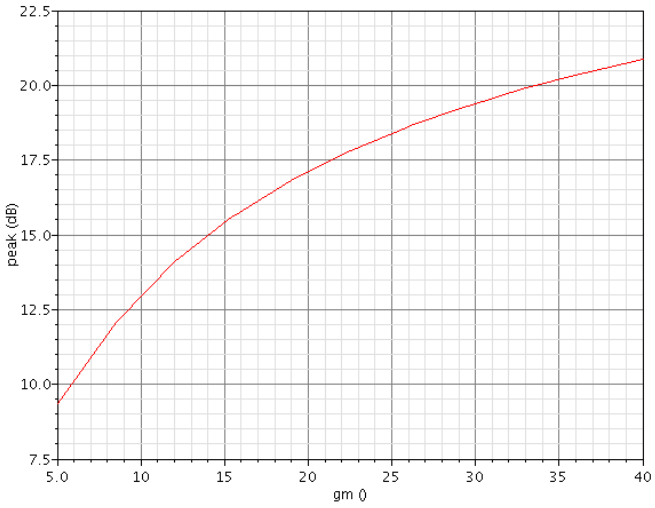

Figure 33: Conversion gain in dB.

For $gm = 20mS$ the gain of the mixer is 17dB, which is a lower than the expected 22dB probably due to the implementation of harmonic rejection and the LO signal not being a perfect square wave.

6.2 Noise performance

In Figure 34 the noise figure of the system as a function of the variable gm can be seen. Since R_D is kept constant, R_E reduces for larger values of gm. And thus, as expected, the noise figure decreases by increasing gm. This is also confirmed by inspection of the noise summary, shown in , which indeed shows that the degeneration resistors R_E and output resistors R_D are dominant noise sources of the system.

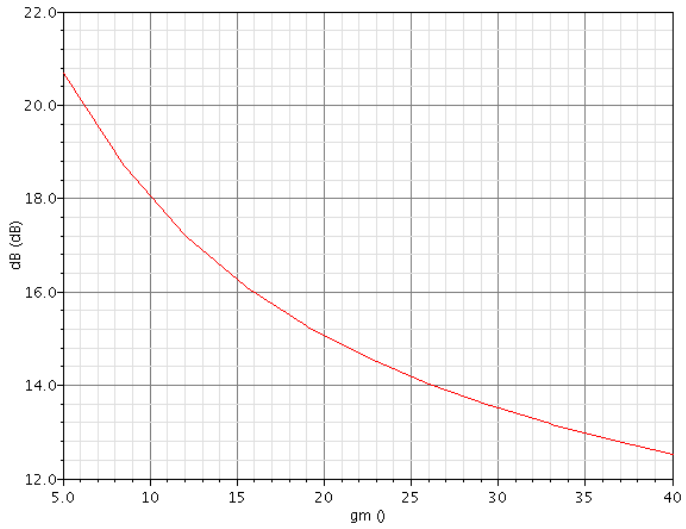

Figure 34: Noise figure in dB.

Table 7: Dominant noise sources of the system.

Noise source	**Number of instances**	**Percentage of total noise**
Resistance input port	1	6.2%
R_D	2	2.5%
R_E (middle cell of HR mixer scaled by 7)	4	2.1%
R_E (outer two cells of HR mixer scaled by 5)	8	1.5%

For $gm = 20$ the noise figure of the mixer is 15dB.

6.3 Linearity

The linearity of the mixer is expressed by the 1dB compression point and the Input referred third-order Intercept Point (IIP3).

The 1dB compression point of the mixer for $gm = 20mS$ is -3.9 dBm, which is shown in Figure 35. The IIP3 of the mixer for $gm = 20mS$ is 5.1 dBm, which is shown in Figure 36.

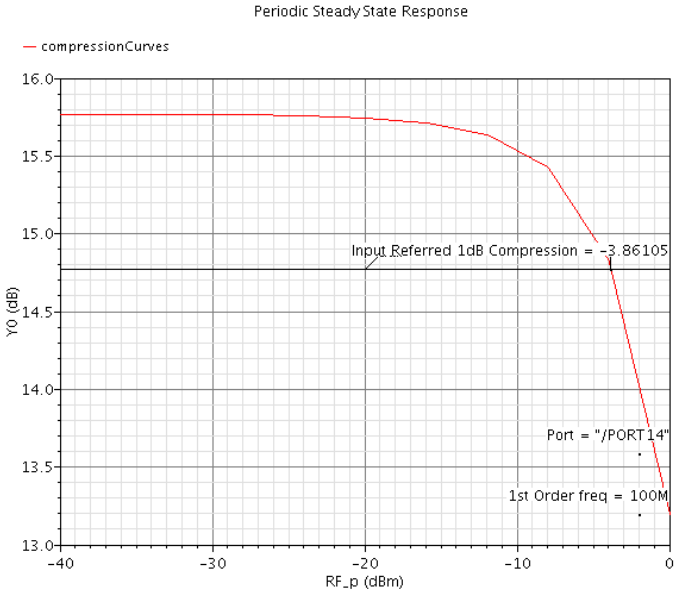

Figure 35: 1dB compression point in dBm.

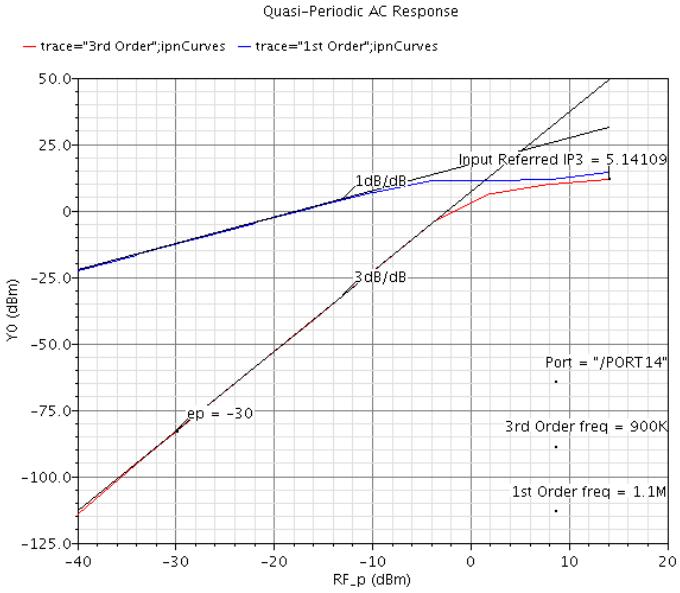

Figure 36: IIP3 in dBm (tones: 2.501GHz and 2.5011GHz).

6.4 Power consumption

The power consumption of the total system as was shown in figure 32 is 122 mW. Since 16 mixers are implemented, the power consumption per mixer is 7.6 mW.

The power consumption is totally dominated by the DC bias current through the resistors, R_D, of the output stage. The power consumption could be reduced by increasing these resistors at the cost of a noise performance degradation.

6.5 Beamforming

To compare the system not implementing beamforming to the same system implementing beamforming a worst-case scenario is considered. That is, the interferer is originating from an angle for which none of the available radiation patterns has a zero. Therefore, the interferer has to be blocked by a beam whose radiation pattern has a zero close to, but not at, the angle the interferer is originating from.

Now, the output of the system (beam) that blocked the interferer most is considered. The magnitude of the wanted signal and the interferer at this output are plotted against the input power level of the interferer. This is done for as well the system not implementing beamforming as the system implementing beamforming. Both times considering the worst case scenario. The input power level of the wanted signal is kept constant at -10 dBm. The plot for the system not implementing beamforming can be seen in Figure 37. The plot for the system implementing beamforming can be seen in Figure 38.

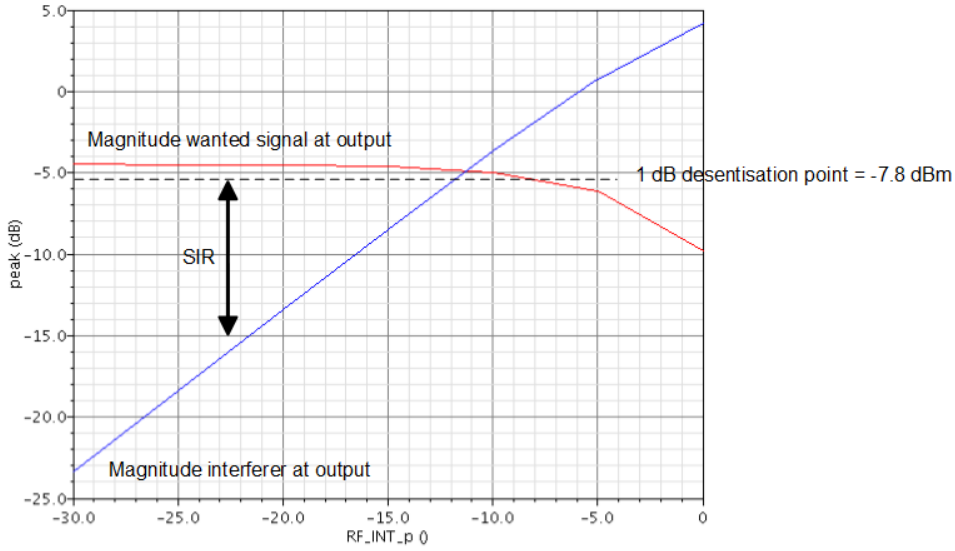

Figure 37: Magnitude of the wanted signal (-10 dBm) and the interferer at the output of the system plotted against the input power level of the interferer. No beamforming implemented.

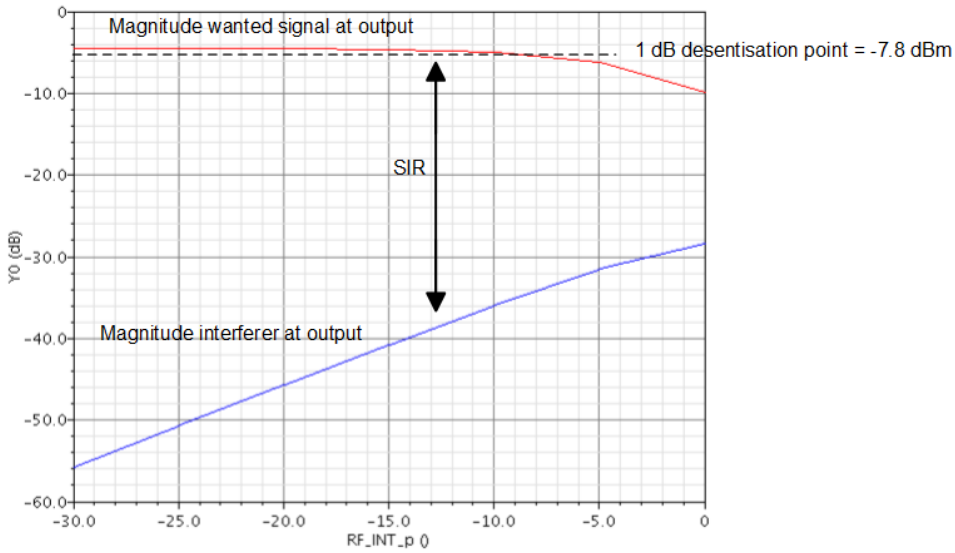

Figure 38: Magnitude of the wanted signal (-10 dBm) and the interferer at the output of the system plotted against the input power level of the interferer. Beamforming implemented.

The figures show that for both systems the 1 dB desensitisation point is -7.8 dBm. The implementation of beamforming did improve the Signal-to-Interferer Ratio (SIR), though. The SIR is improved by 33 dB by implementing beamforming.

The improvement of the SIR of the system is translated to an improvement in the 1 dB desensitisation point if some gain after beamforming is considered. The improvement in the SIR will then prevent the interferer from desensitising the amplifier implementing this gain.

As an example, for the next two plots the scenario is considered where 20 dB gain is added after the mixer (and possible beamforming) block and the input

power level is 20 dBm lower. For this scenario, the plot for the system not implementing beamforming can be seen in Figure 39. And the plot for the system implementing beamforming can be seen in Figure 40.

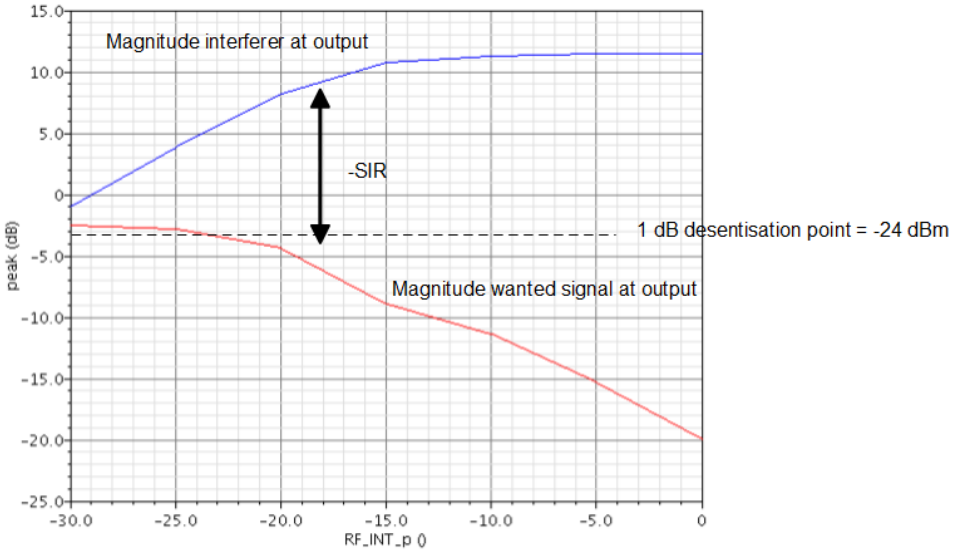

Figure 39: Magnitude of the wanted signal (-30 dBm) and the interferer at the output of the system plotted against the input power level of the interferer. No beamforming implemented, 20 dB gain added.

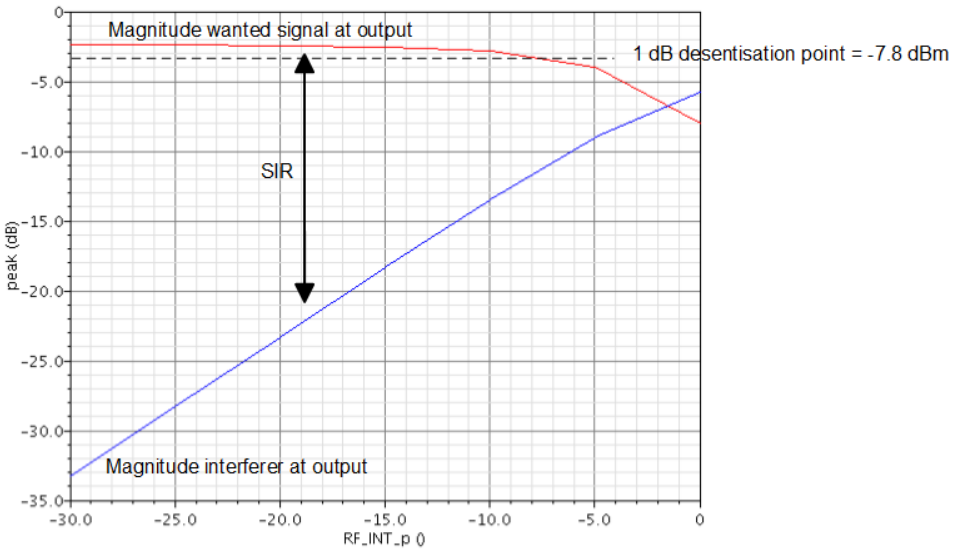

Figure 40: Magnitude of the wanted signal (-30 dBm) and the interferer at the output of the system plotted against the input power level of the interferer. Beamforming implemented, 20 dB gain added.

Now, the 1 dB desensitisation point of the system not implementing beamforming is -24 dBm, whereas the 1 dB desensitisation point of the system implementing beamforming is still -7.8 dBm. So, the 1 dB desensitisation point of the system is improved with 16 dBm by implementing beamforming. Since the input power level of the wanted signal is lowered to 30 dBm for this scenario,

naturally the SIR for both systems is decreased. The SIR is still improved by 33 dB by implementing beamforming, though.

The goal of this research is for an interferer to affect as little beams as possible, ideally only one. The other three beams should therefore all show an improvement in SIR. The system level simulation in section 4.1 showed that for all the three beams the improvement in SIR should be at least 14dB. For the worst-case scenario the beam with the least SIR improvement, apart from the beam that 'captured' the interferer, showed an SIR improvement of 14.1dB. This is in accordance with the expectation from the system level simulations.

7 Conclusions

The goal of this research is to design an RF frontend for a digital beamforming Software Defined Radio Receiver, that implements initial beamforming. The initial beamforming should reject interferers, while preserving as much of the information from the input signals as possible, so further beamforming can be performed in software. Therefore four beams are created of which, ideally, only one is affected by the interferer.

- Beams can be constructed by summing the input signals of the elements of an antenna array with phase weights. In this thesis a 4 element antenna array is used. If any beam that can be constructed by a phase-weighted sum of the input signals of this array (the phase-weighted beams), can also be constructed by a linear combination of a certain set of 4 beams, then this set of 4 beams is a basis for all phase-weighted beams. It is proven in section 2.2 that any set of 4 phase-weighted orthogonal beams is a basis for all phase-weighted beams.

- Given any phase-weighted beam, a set of 4 orthogonal beams can be created by shifting the first beam in u-space by $\frac{1}{2}$, 1 and $\frac{3}{2}$ to create the second, third and fourth beam, respectively.

- Two beamforming strategies are investigated. The first strategy applies a uniformly increasing phase shift to the input signals, resulting in one fixed beamshape that is shifted in u-space. The second strategy placed no constraints on the applied phase shifts, resulting in varying beamshapes shifted in u-space. The two strategies are compared using two figures of merit described in section 4.1. The variable beamshape strategy showed better overall performance.

- The extra LO phases that are created for harmonic rejection can be exploited to implement beamforming by adding some routing circuitry. This way, dedicated phase shifters for beamforming can be saved. For harmonic rejection 8 phase-shifted copies of the input signals are created by mixing the input signal with 8 LO phases. Using these 8 mixer outputs to implement beamforming the performance will be equal to when implementing beamforming with 3 bit phase shifters.

- System evaluations showed that the variable beamshape strategy can reject interferers from any angle up to 14 dBFS (normalised to the voltage range of the ADC after amplification) when implemented with 3 bit phase shifters.

- The phase-shifted copies of an input signal are created by 4 double-balanced mixers driven by 4 LO phases. Also using the outputs of these mixers with reversed polarity results in the 8 available phase-shifted copies of the input signal. Exploiting the fact that any common phase shift applied to the signals constituting a beam does not alter the radiation pattern, a beam construction matrix can be obtained in which every mixer output is only used once. Therefore, the variable beamshape strategy with 8 phases can be implemented using only 4 differential mixers.

- The routing circuitry needed for beamforming can be implemented by adding 8 switches to the output of each mixer. This first four switches route the current of each mixer to one of the four beams (outputs). The other four switches are used to route the current to the four beams with reversed polarity.

- Considering a worst-case scenario, implementing beamforming achieves a 33 dB improvement in SIR for the beam rejecting the interferer most in comparison to when no beamforming is implemented. The beam with the least SIR improvement, apart from the beam that 'captured' the interferer, showed an SIR improvement of 14.1dB.

8 Recommendations

- Because beamforming only happens after downconversion, a very strong interferer could desensitise the LNA. This could be avoided by using the mixer as the first block in de the receiver. The noise figure of the implemented beamforming mixer is too high to be used in a mixer-first design, though. That is, the mixer has to be preceded by an LNA. This is because according to Friis' formula (Friis 1944) in equation 8.1 the overall noise figure of a radio receiver is primarily determined by the noise figure of the first amplifying stage.

$$F_{total} = F_1 + \frac{F_2 - 1}{G_1} + \frac{F_3 - 1}{G_1 G_2} + \cdots + \frac{F_n - 1}{G_1 G_2 \ldots G_{n-1}} \quad (8.1)$$

  It can be investigated if the variable beamshape strategy can be implemented in a different mixer topology that has a better noise performance. For example (Andrews en Molnar 2010) propose a mixer-first topology that achieves a noise figure of <6 dB and also provides 8 LO phase outputs.

Bibliography

Buracchin, Enrico. 2000. “The Software Radio Concept.” *Communications Magazine, IEEE* 138-143.

Butler, J, and R Lowe. 1961. “Beam-forming matrix simplifies design of electrically scanned antennas.” *Electronic Design* 170-173.

Friis, H.T. 1944. “Noise Figures of Radio Receivers.” *Proceedings of the IRE* 419-422 .

Gilbert, Barrie Barrie. 1968. “A precise four-quadrant multiplier with subnanosecond response.” *Solid-State Circuits, IEEE Journal of* 365-373.

Griffiths, David J. 2005. *Introduction to quantum mechanics.* Pearson.

Jing Zhu, Alan Waltho, Xue Yang, and Xingang Guo. 2007. “Multi-Radio Coexistence: Challenges and Opportunities.” *Computer Communications and Networks, 2007. ICCCN 2007. Proceedings of 16th International Conference on* 358-364.

Klumperink, E.A.M. 2007. “Cognitive radios for dynamic spectrum access - polyphase multipath radio circuits for dynamic spectrum access.” *Communications Magazine, IEEE* 104-105.

Paramesh, Jeyanandh. 2005. “A 1.4V 5GHz four-antenna Cartesian-combining receiver in 90nm CMOS for beamforming and spatial diversity applications.” *Solid-State Circuits Conference, 2005. Digest of Technical Papers. ISSCC. 2005 IEEE International.* Hillsboro. 210-594.

Ru, Z., N.A. Moseley, E. Klumperink, and B. Nauta. 2009. “Digitally Enhanced Software-Defined Radio Receiver Robust to Out-of-Band Interference.” *Solid-State Circuits, IEEE Journal of* (Solid-State Circuits, IEEE Journal of) 3359-3375.

Shen, Dongjun. 2011. “A 2.4 GHz Low Power Folded Down-conversion Quadrature Mixer in 0.18-µm CMOS.” *Wireless Communications and Signal Processing (WCSP), 2011 International Conference on.* 1-4.

2013. *STARS - Theme 2: Analog Front-Ends.* February. http://starsproject.nl/activities/theme2/.

Sulivan, P.J. 1997. “Low voltage performance of a microwave CMOS Gilbert cell mixer.” *Solid-State Circuits, IEEE Journal of* 1151-1155.

van den Ende, F., M.C.M. Soer, E.A.M. Klumperink, and F.E. van Vliet. 2011. *Interference Nulling via a Resistor-Weighted Op-Amp Vector Modulator.* Enschede: University of Twente.

Visser, Hubregt J. 2005. In *Array and Phased Array Antenna Basics*. Wiley.

Weldon, J.A. 2005. *High Performance CMOS Transmitters for Wireless Communications .* PhD Thesis, Berkeley: UNIVERSITY OF CALIFORNIA, BERKELEY .

Weldon, Jeffrey A. 2001. “A 1.75-GHz highly integrated narrow-band CMOS transmitter with harmonic-rejection mixers.” *Solid-State Circuits, IEEE Journal of.* 2003-2015.

Appendix A

```
clear all;

% Number of steps to simulate. Increase for better precision.
steps = 501;

% Some constants
pi = 3.141592;
c = 299792458;

% Carrier frequency and possibility to introduce beam squint.
f_c = 2.4 * 10^9;
f_s = 2.4 * 10^9;

% Define the array factor as a matrix
lambda_0 = c / f_c;
lambda_s = c / f_s;

k0 = 2 * pi / lambda_s;
d = 0.5 * lambda_0;

u = -1: 2/(steps - 1) : 1;
n = [1;2;3;4];
phi = k0 * (n - 1) * d * u;
S = exp(1i * phi);

% Normalized magnitude of the interferer.
mag_int = 10;

% Number of interferer angles to simulate for.
int_steps = 180;

% The values for both methods to sweep over.
M1_sweep = 2:4;
M2_sweep = 2:4;

% Pre-allocate arrays to increase speed of the simulation.
% Later on reshape, repmat and bsxfun are used. Once again for performace
% issues. These functions are optimized for multiple cores and speed up the
% simulation.
M1_Pavg = zeros(2^max(M1_sweep), int_steps, size(M1_sweep,2));
M1_Pdesired = zeros(2^max(M1_sweep), int_steps, size(M1_sweep,2));
M2_Pavg = zeros(2^max(M2_sweep)^3, int_steps, size(M2_sweep,2));
M2_Pdesired = zeros(2^max(M2_sweep)^3, int_steps, size(M2_sweep,2));

% Define the standard 4 beams.
B_0 = exp(1i * [0 0 0 0;
       0 1 0 1;
       0 1.5 1 0.5;
       0 0.5 1 1.5] * pi) / 4;

n = 0;
% Loop through all bits.
for bits = M1_sweep
    n = n + 1;

    i = 0;
    % Loop through all possible phase shifts.
```

```
    for rot = 0 : 2^bits
        i = i + 1;

        a = 4 * rot * (180 / 2^bits);
        b = 3 * rot * (180 / 2^bits);
        c = 2 * rot * (180 / 2^bits);
        d = 1 * rot * (180 / 2^bits);

        PSI = exp(1i * [a b c d;
           a b c d;
           a b c d;
           a b c d] * pi);

        % Apply phase shift.
        beams = (B_0 .* PSI) * S;

        int_vector = ceil((1/int_steps : 1/int_steps : 1) * steps);
        w = 1./max(abs(beams(:,int_vector))*mag_int,1);

        % Discard beam if it is too large for the ADC.
        mags = floor(w .* 2^0) / 2^0;
        mags_r = reshape(mags, 4 * int_steps, 1);

        beams_r = repmat(beams, int_steps, 1);
        weighted_beams = bsxfun(@times, mags_r, beams_r);

        % Loop through all interferer angles and define the FOMs for this phase
        % shift and all interferers.
        for k = 1 : int_steps
            phase_correction = [1; 1; 1; 1];
            beam_slice = bsxfun(@times, phase_correction, weighted_beams(4*(k - 1) +
(1:4),1:end));

            AF = abs(sum(beam_slice));

            % Define FOMs for this phase shift
            M1_Pavg(i,k,n) = sum(AF) / steps;
            M1_Pdesired(i,k,n) = AF(ceil(steps/2));
        end
    end
end

n = 0;
% Loop though all number of LO phases.
for angle_steps = 2.^M2_sweep
    n = n + 1;
    angles = 0:2/angle_steps:2-2/angle_steps;

    i = 0;
    % Loop through all variable beamshapes.
    for a = 0
        for b = angles
            for c = angles
                for d = angles
                    i = i + 1;

                    %RB = (9.5*ones(4,4)+rand(4,4))/10;

                    B_0 = exp(1i * [a b c d;
                        (a + 0.25) (b + 0.75) (c + 1.25) (d + 1.75);
```

```
                        (a + 0.50) (b + 1.50) (c + 0.50) (d + 1.50);
                        (a + 0.75) (b + 0.25) (c + 1.75) (d + 1.25)] * pi) / 4;

                    beams = B_0 * S;

                    int_vector = ceil((1/int_steps : 1/int_steps : 1) * steps);
                    w = 1./max(abs(beams(:,int_vector))*mag_int,1);

                    mags = floor(w .* 2^0) / 2^0;
                    mags_r = reshape(mags, 4 * int_steps, 1);

                    beams_r = repmat(beams, int_steps, 1);
                    weighted_beams = bsxfun(@times, mags_r, beams_r);

                    % Loop through all interferer angles and define the
                    % FOMs for this variable beamshape and all interferers.
                    for k = 1 : int_steps
                        phase_correction = exp(1i * [0; 0.25; 0.5; 0.75] * pi);
                        beam_slice = bsxfun(@times, phase_correction,
weighted_beams(4*(k - 1) + (1:4),1:end));

                        AF = abs(sum(beam_slice));
                        M2_Pavg(i,k,n) = sum(AF) / steps;
                        M2_Pdesired(i,k,n) = AF(ceil(steps/2));
                    end
                end
            end
        end
    end
end

% Plot the results of the simulation
figure
subplot(2,3,1);
plot(-1:2/(int_steps-1):1, 20*log10(max(M1_Pavg(:,:,1))))
axis([-1 1 -10 0]);
title('Fixed beamshape strategy - Pavg - 2 bits phase shifter')
xlabel('Angle of incidence of interferer - u []')
ylabel('PT [dB]')

% …
% …
% …

subplot(2,3,6);
plot(-1:2/(int_steps-1):1, 20*log10(max(M2_Pdesired(:,:,3))))
title('Variable beamshape strategy - Pdesired - 4 bits phase shifter)
xlabel('Angle of incidence of interferer - u []')
ylabel('P0 [dB]')
```